Dual-Polarized Ricean MIMO Channels: Modeling and Performance Assessment

Adrian Ispas, *Student Member, IEEE*, Xitao Gong, *Student Member, IEEE*, Christian Schneider, Gerd Ascheid, *Senior Member, IEEE*, and Reiner Thomä, *Fellow, IEEE*

***Abstract*—In wireless communication systems, dual-polarized (DP) instead of single-polarized (SP) multiple-input multiple-output (MIMO) transmission is used to improve the spectral efficiency under certain conditions on the channel and the signal-to-noise ratio (SNR). In order to identify these conditions, we first propose a novel channel model for DP mobile Ricean MIMO channels for which statistical channel parameters are readily obtained from a moment-based channel decomposition. Second, we derive an approximation of the mutual information (MI), which can be expressed as a function of those statistical channel parameters. Based on this approximation, we characterize the required SNR for a DP MIMO system to outperform an SP MIMO system in terms of the MI. Finally, we apply our results to channel measurements at 2.53 GHz. We find that, using the proposed channel decomposition and the approximation of the MI, we are able to reproduce the SNR values above which DP MIMO systems outperform SP MIMO systems.**

***Index Terms*—Channel models, MIMO, performance evaluation, Rician channels**

I. Introduction

MULTIPLE-input multiple-output (MIMO) transmission is by now a well established technique to enhance the spectral efficiency over wireless channels. While commonly antennas with the same polarization are considered for MIMO systems, the use of dual-polarized (DP) antennas is known to offer advantages in terms of the spectral efficiency under certain conditions on the channel and the signal-to-noise ratio (SNR). Besides being able to improve the spectral efficiency, DP antennas allow for compact MIMO systems with co-located antennas due to the strong decorrelation over orthogonal polarizations.

In order to understand the influence of channel properties and the SNR on the spectral efficiency, channel models are commonly used. The main goal of channel models is to give a simplified yet accurate representation of the effects of the channel on the transmitted signal. They thus allow to replace the use of sophisticated channel measurements that are specific to a measurement environment, and, furthermore, they can allow for analytical evaluations. A good overview on the modeling of DP MIMO channels can be found in [1]–[3]. Experimental results regarding DP MIMO channels are presented in, e.g., [2], [4]–[6]. Furthermore, in [7], the orthogonality of DP MIMO channels is characterized, and, in [8], the impact of Ricean fading channels on the diversity performance is investigated analytically.

Unfortunately, an accurate and analytically tractable modeling of DP MIMO channels is a difficult task. One has to resort to several assumptions in order to obtain analytical expressions, e.g., for the mutual information (MI), and thus to assess the influence of the channel on the spectral efficiency. It is known that DP MIMO systems are attractive in Ricean channels [2], [9]. However, the channel and the SNR conditions for a DP MIMO system to outperform a single-polarized (SP) MIMO system in terms of the spectral efficiency are not fully characterized and they are time-dependent. Expressions relating the statistical channel parameters to the spectral efficiency are usually limited to restrictive channel models with separable correlation, i.e., a Kronecker structure, and/or without a Ricean component; moreover, they often rely on asymptotic settings. For recent contributions regarding analytical expressions of the MI for Ricean channels in asymptotic settings, see [10] and references therein. The dependence of the spectral efficiency of SP and DP MIMO channels on the SNR and the K-factor is demonstrated, e.g., in [1] with simulated channels. The spectral efficiency of measured SP and DP MIMO channels with (instantaneous) channel state information (CSI) at the receiver (RX) only has been compared, e.g., in [11] with indoor measurements at 2.4 GHz, in [12] with indoor measurements at 1.95 GHz, or in [13] with outdoor measurements at 2.5 GHz. While [12] and [13] conclude that DP MIMO systems are favorable, [11] concludes that, especially for low K-factors, SP MIMO systems are recommended to reach higher spectral efficiencies. Therefore, as highlighted in [4], it is not straightforward to decide when to use a DP instead of an SP MIMO system. We also note that SP MIMO systems would highly benefit from the availability of CSI at the transmitter (TX). Apart from instantaneous CSI, which is challenging to obtain in practice, statistical CSI at the TX or the use of codebooks with limited feedback to the TX can also provide gains in spectral efficiency that are easier to realize, see, e.g., [14]–[17].

We first aim at establishing a general channel model for SP and DP MIMO systems which is reasonably accurate, yet analytically tractable. Second, we aim at identifying the

This work was supported by the Ultra high-speed Mobile Information and Communication (UMIC) research centre. Parts of this work were presented at the IEEE Global Communications Conference (GLOBECOM), Anaheim, CA, USA, December 2012.

Adrian Ispas was with the Chair for Integrated Signal Processing Systems, RWTH Aachen University. He is now with Rohde & Schwarz GmbH & Co. KG, 81671 Munich, Germany (e-mail: ispas@iss.rwth-aachen.de).

Xitao Gong and Gerd Ascheid are with the Chair for Integrated Signal Processing Systems, RWTH Aachen University, 52056 Aachen, Germany (e-mail: {gong, ascheid}@iss.rwth-aachen.de).

Christian Schneider and Reiner Thomä are with the Institute for Information Technology, Ilmenau University of Technology, 98684 Ilmenau, Germany (e-mail: {christian.schneider, reiner.thomae}@tu-ilmenau.de).

conditions on the channel and the SNR under which it is beneficial, in terms of spectral efficiency, to make use of the polarization domain for a limited number of antennas at both link ends. The reason to limit the number of simultaneously used antennas is that it is desirable to keep a low number of radio frequency chains since they are expensive components in a wireless system. One can then perform antenna switching between differently polarized antennas, i.e., between SP and DP MIMO systems.

Contributions: We detail a general modeling approach for SP and DP MIMO channels. Furthermore, we evaluate the achievable rate over such channels for the case that the TX has only statistical CSI, while the RX has instantaneous CSI. In particular, we contribute the following:

- We propose a general model for SP and DP mobile Ricean MIMO channels. Furthermore, we derive a moment-based channel decomposition yielding the statistical channel model parameters from measured data.
- We give an approximation of the achievable rate, i.e., the MI, which is an explicit function of the statistical parameters of the proposed channel model. We can thus assess the influence of the statistical channel parameters on the achievable rate.
- We use the approximate MI to characterize the required SNR for a DP setup to outperform an SP setup. Specifically, we give a closed-form expression of such an SNR threshold for the practically relevant case of a dual-stream DP setup vs. a single-stream SP setup.
- We evaluate the channel decomposition and the MI for 4×4 SP and DP MIMO systems based on urban macrocell measurements at 2.53 GHz. We find that the DP setup is advantageous in terms of the MI for medium- to high-K-factor links above a certain SNR. With the approximate evaluation of the MI, we can reproduce the crossing points between the MI of the SP and DP MIMO systems.

Structure: We first introduce the MIMO system model in Section II. Then, in Section III, we develop the channel model and its corresponding decomposition technique for SP and DP channels. Section IV deals with the performance assessment for SP and DP MIMO transmission. In Section V, the channel measurements and the data selection are presented, before proceeding with the results in Section VI. Finally, we draw the conclusion in Section VII.

Notation: We use lowercase and uppercase boldface letters to designate vectors and matrices, respectively. For a matrix $\mathbf{A}$, the (element-wise) complex conjugate, the transpose, and the conjugate transpose are denoted by $\mathbf{A}^*$, $\mathbf{A}^T$, and $\mathbf{A}^H$, respectively. The unique Hermitian positive semidefinite square root of a Hermitian positive semidefinite matrix $\mathbf{A}$ is represented by $\mathbf{A}^{\frac{1}{2}}$. For the matrix $\mathbf{A}$, $\mathrm{tr}\{\mathbf{A}\}$, $\mathrm{rank}\{\mathbf{A}\}$, and $\lambda_{\max}(\mathbf{A})$ denote the trace, the rank, and the maximal eigenvalue, respectively. For two matrices $\mathbf{A}$ and $\mathbf{B}$, $\mathbf{A}\odot\mathbf{B}$ is the Hadamard (element-wise) product and $\mathbf{A}\otimes\mathbf{B}$ is the Kronecker product. The vectorization, i.e., the column-wise stacking, of the matrix $\mathbf{A}$ is denoted by $\mathrm{vec}\{\mathbf{A}\}$. The $N\times N$ identity matrix is represented by $\mathbf{I}_N$ and the all-zero matrix of size $N_1\times N_2$ is denoted by $\mathbf{0}_{N_1,N_2}$. The real-valued $MN\times MN$ commutation matrix $\mathbf{K}_{M,N}$ satisfies $\mathbf{K}_{M,N}\,\mathrm{vec}\{\mathbf{A}\}=\mathrm{vec}\{\mathbf{A}^T\}$ for an $M\times N$ matrix $\mathbf{A}$. Consider an $M\times N$ matrix $\mathbf{A}$ with $k=1,\ldots,M$ and $l=1,\ldots,N$; we use $[\mathbf{A}]_{k,l}$ to denote the element in the kth row and the lth column of $\mathbf{A}$, and we define $\mathbf{A}^+$ such that $[\mathbf{A}^+]_{k,l}=\max\{[\mathbf{A}]_{k,l},0\}$ holds. Expectation is denoted by $\mathrm{E}\{\cdot\}$, $\log(\cdot)$ is the logarithm to the base 2, and $\ln(\cdot)$ is the natural logarithm. The imaginary unit is represented by j.

II. System Model

We consider a MIMO channel which is characterized by time-varying and frequency-flat fading. The input-output relation for transmission from N_{TX} antennas at the TX to N_{RX} antennas at the RX is given at time slots $m\in\mathbb{Z}$ by the received length-N_{RX} column vector

$$\mathbf{y}[m]=\mathbf{H}[m]\mathbf{x}[m]+\mathbf{n}[m]. \tag{1}$$

The random channel matrices $\{\mathbf{H}[m]\}$, each of size $N_{\mathrm{RX}}\times N_{\mathrm{TX}}$, are jointly proper. The length-N_{TX} column vectors $\{\mathbf{x}[m]\}$ denote the zero-mean jointly proper Gaussian transmitted vectors that are uncorrelated in time with spatial covariance matrix $\mathrm{E}\{\mathbf{x}[m]\mathbf{x}^H[m]\}=P_x\mathbf{Q}[m]$, $P_x>0$, and $\mathrm{tr}\{\mathbf{Q}[m]\}=1$. The length-$N_{\mathrm{RX}}$ column vectors $\{\mathbf{n}[m]\}$ are the white jointly proper Gaussian noise vectors in time with spatial covariance matrix $\mathrm{E}\{\mathbf{n}[m]\mathbf{n}^H[m]\}=\sigma_n^2\mathbf{I}_{N_{\mathrm{RX}}}$ and $\sigma_n^2>0$. The random processes $\{\mathbf{H}[m]\}$, $\{\mathbf{n}[m]\}$, and $\{\mathbf{x}[m]\}$ are assumed to be mutually independent. For ease of exposition, we define the (nominal) SNR $\rho=P_x/\sigma_n^2$. We assume the RX to have instantaneous CSI, i.e., the RX has knowledge of the current channel realization $\mathbf{H}[m]$. The TX, on the other hand, only has statistical CSI of the channel.

III. Channel Modeling and Decomposition

A channel model has to be accurate yet simple enough to offer insight on the influence of the relevant channel parameters on the system performance. Several approaches to model the channel exist; they can be mainly classified in physical and analytical models [18]. While analytical channel models describe the propagation environment and the antennas, for physical channel models the antenna arrays need to be included in an additional step [19], [20]. We choose the correlation-based analytical modeling approach for MIMO channels since it allows for analytical evaluations and requires statistical parameters that are, in general, readily available from measurement data. Correlation-based models are characterized by a multivariate proper Gaussian term representing the joint effects of a large number of independent scatterers. When additionally a dominant channel component is present due to a line-of-sight (LOS) connection or a strong scatterer, one usually defines the ratio between the power of the dominant component and the power of the remaining weaker components as the K-factor.

A. Channel Model

It is common to represent the dominant components of the MIMO channel by a deterministic rank-one matrix [21], [22]. While this is usually applicable for an SP MIMO system in

an LOS scenario where the TX and the RX are fixed, it is not appropriate in general. This is especially true for DP MIMO systems where independent propagation along orthogonal polarizations might occur. Moreover, in the presence of a mobile terminal (MT), a dominant channel component, due to, e.g., a strong scatterer or a LOS connection, has a varying phase and as a consequence the mean of the channel is zero [23], [24].[1] We thus introduce the following model for SP and DP mobile MIMO channels:

$$\mathbf{H}[m] = \underbrace{\begin{bmatrix} \bar{\mathbf{H}}_{\mathrm{VV}}[m] & \bar{\mathbf{H}}_{\mathrm{HV}}[m] \\ \bar{\mathbf{H}}_{\mathrm{VH}}[m] & \bar{\mathbf{H}}_{\mathrm{HH}}[m] \end{bmatrix}}_{=\bar{\mathbf{H}}[m]} + \underbrace{\begin{bmatrix} \tilde{\mathbf{H}}_{\mathrm{VV}}[m] & \tilde{\mathbf{H}}_{\mathrm{HV}}[m] \\ \tilde{\mathbf{H}}_{\mathrm{VH}}[m] & \tilde{\mathbf{H}}_{\mathrm{HH}}[m] \end{bmatrix}}_{=\tilde{\mathbf{H}}[m]} \quad (2)$$

where $\bar{\mathbf{H}}[m]$ contains the dominant contributions, which are due to LOS or strong scatterers, and $\tilde{\mathbf{H}}[m]$ contains the remaining contributions of the channel. The $N_{\mathrm{RX},b} \times N_{\mathrm{TX},a}$ sub-matrices

$$\bar{\mathbf{H}}_{ab}[m] = \mathbf{V}_{ab}[m] \odot \mathbf{\Phi}_{ab}[m] \quad (3)$$

and $\tilde{\mathbf{H}}_{ab}[m]$ contain the sub-links with polarization a at the TX and b at the RX for $a, b \in \{\mathrm{V}, \mathrm{H}\}$. Here, V and H denote vertical and horizontal polarizations, respectively.[2] The number of vertical-polarized (VP) and the number of horizontal-polarized (HP) antennas at the TX are given by $N_{\mathrm{TX,V}}$ and $N_{\mathrm{TX,H}}$, respectively. We thus have $N_{\mathrm{TX,V}} + N_{\mathrm{TX,H}} = N_{\mathrm{TX}}$. The relations at the RX side are obtained analogously. In the SP case, we either use only VP or only HP antennas. In the DP case, we assume that, at both the TX and the RX, one half of the antennas is VP while the other half is HP. We split the dominant contributions into the deterministic amplitude matrix $\mathbf{V}_{ab}[m]$ and the random phase matrix $\mathbf{\Phi}_{ab}[m]$ with $[\mathbf{\Phi}_{ab}[m]]_{k,l} = e^{j\phi_{ab,(l-1)N_{\mathrm{RX},b}+k}[m]}$ for $k = 1, \ldots, N_{\mathrm{RX},b}$ and $l = 1, \ldots, N_{\mathrm{TX},a}$. The remaining weaker scatterers are represented by the zero-mean proper Gaussian matrix $\tilde{\mathbf{H}}[m]$, i.e., $\tilde{\mathbf{H}}_{ab}[m]$ for $a, b \in \{\mathrm{V}, \mathrm{H}\}$. As highlighted in [3], the challenging part is the modeling of the dependence between the phases of the dominant components $\phi_{ab,p}[m]$ for $p = 1, \ldots, N_{\mathrm{TX},a}N_{\mathrm{RX},b}$. We first consider all MIMO sub-links with polarization a at the TX and b at the RX. For $p, q = 1, \ldots, N_{\mathrm{TX},a}N_{\mathrm{RX},b}$, we assume

1) $\phi_{ab,p}[m]$ is independent of $\tilde{\mathbf{H}}[m]$,
2) $\phi_{ab,p}[m]$ is uniformly distributed over $[-\pi, \pi)$,
3) $\Delta^{p,q}_{\phi,ab}[m] = \phi_{ab,p}[m] - \phi_{ab,q}[m]$ is deterministic.

The first two assumptions are commonly used, see, e.g., [3]. However, a note is in order regarding the last assumption. As mentioned above, the contributions from the dominant components are not deterministic, e.g., due to the mobility of the MT. For the case that all MIMO sub-links of the same polarization combination a and b observe the same dominant component and that the distances between the TX, the RX, and a possible dominant scatterer are considerably larger than the array sizes, the resulting phase changes are equal for all of these sub-links. Therefore, $\Delta^{p,q}_{\phi,ab}[m]$ is modeled as deterministic. Significant variations related to the dominant component, e.g., due to the movement of the MT, will result in a change of $\Delta^{p,q}_{\phi,ab}[m]$ and thus in a change of the channel statistics. Clearly, assumption 3) is not satisfied for all antenna setups, e.g., it would not necessarily hold for a MIMO system made of directional antennas with different orientations. Therefore, for each polarization, we require the (directional) antennas at the TX and the RX to be oriented in the same direction. Using assumption 3), we can rewrite (3) as

$$\bar{\mathbf{H}}_{ab}[m] = \mathbf{V}_{ab}[m] \odot \mathbf{\Delta}_{\phi,ab}[m]\ e^{j\phi_{ab}[m]},\ a, b \in \{\mathrm{V}, \mathrm{H}\} \quad (4)$$

where we defined $\phi_{ab}[m] = \phi_{ab,1}[m]$ and the deterministic matrix $\mathbf{\Delta}_{\phi,ab}[m] = \mathbf{\Phi}_{ab}[m]\ e^{-j\phi_{ab}[m]}$. We can thus have one dominant component per polarization component, where each dominant component can have different angles of departure/arrival.

B. Channel Correlation

Subsequently, we define full and transmit correlation matrices of the channel. Furthermore, we characterize the structure of the correlation matrices of the dominant components of the channel. The results will be needed for the channel decomposition in Section III-C and the performance assessment in Section IV.[3]

1) Full Channel Correlation Matrices: We first define the length-$N_{\mathrm{TX}}N_{\mathrm{RX}}$ column vectors $\mathbf{h}[m] = \mathrm{vec}\{\mathbf{H}[m]\}$, $\bar{\mathbf{h}}[m] = \mathrm{vec}\{\bar{\mathbf{H}}[m]\}$, and $\tilde{\mathbf{h}}[m] = \mathrm{vec}\{\tilde{\mathbf{H}}[m]\}$. The corresponding $N_{\mathrm{TX}}N_{\mathrm{RX}} \times N_{\mathrm{TX}}N_{\mathrm{RX}}$ full correlation matrices of the channel are then obtained as

$$\mathbf{R}[m] = \mathrm{E}\left\{\mathbf{h}[m]\mathbf{h}^H[m]\right\} \quad (5)$$

$$\bar{\mathbf{R}}[m] = \mathrm{E}\left\{\bar{\mathbf{h}}[m]\bar{\mathbf{h}}^H[m]\right\} \quad (6)$$

$$\tilde{\mathbf{R}}[m] = \mathrm{E}\left\{\tilde{\mathbf{h}}[m]\tilde{\mathbf{h}}^H[m]\right\} \quad (7)$$

respectively. Using assumption 1) in Section III-A, it immediately follows that

$$\mathbf{R}[m] = \bar{\mathbf{R}}[m] + \tilde{\mathbf{R}}[m] \quad (8)$$

holds. We can categorize the MIMO sub-links into co-polarized sub-links, i.e., links with VP to VP or HP to HP transmission, and into cross-polarized sub-links, i.e., links with VP to HP or HP to VP transmission. Depending on whether the four polarizations combinations share a dominant component or not, the rank of $\bar{\mathbf{R}}[m]$ can vary. We show in Appendix A that generally we have $\mathrm{rank}\left\{\bar{\mathbf{R}}[m]\right\} \leq 4$. Since the cross-polarized sub-links are less affected by, e.g., the occurrence of a LOS component [7], we consider the practically relevant setting that only the co-polarized sub-links can be affected by

[1] Another reason for a zero-mean channel can be the consideration of channel samples at other frequencies as different channel realizations.

[2] We note that other polarization choices, e.g., corresponding to a slanted scheme, are possible as well; however, we choose vertical and horizontal polarizations as they often have different propagation characteristics, see [12] for an example in an indoor scenario. Rotations in the antenna arrays can also be accounted for; they will directly influence the statistical channel parameters but not the model structure.

[3] We do not investigate RX channel correlation matrices since those are not needed for the channel decomposition or the performance assessment.

dominant components.[4] Then, it can be similarly shown that $\mathrm{rank}\left\{\bar{\mathbf{R}}[m]\right\} \leq 2$ has to be satisfied. Further specializing this setting to the case that the VP to VP and the HP to HP sub-links are affected by distinct dominant components with independent phase terms, it follows that $\mathrm{rank}\left\{\bar{\mathbf{R}}[m]\right\} = 2$ is satisfied. When all polarization combinations share a common dominant component, we have $\mathrm{rank}\left\{\bar{\mathbf{R}}[m]\right\} = 1$. For an SP setup, $\mathrm{rank}\left\{\bar{\mathbf{R}}[m]\right\} \leq 1$ holds.

2) Transmit Channel Correlation Matrices: The $N_{\mathrm{TX}} \times N_{\mathrm{TX}}$ TX correlation matrices are

$$\mathbf{R}_{\mathrm{TX}}[m] = \mathrm{E}\left\{\mathbf{H}^T[m]\mathbf{H}^*[m]\right\} \tag{9}$$

$$\bar{\mathbf{R}}_{\mathrm{TX}}[m] = \mathrm{E}\left\{\bar{\mathbf{H}}^T[m]\bar{\mathbf{H}}^*[m]\right\} \tag{10}$$

$$\tilde{\mathbf{R}}_{\mathrm{TX}}[m] = \mathrm{E}\left\{\tilde{\mathbf{H}}^T[m]\tilde{\mathbf{H}}^*[m]\right\}. \tag{11}$$

With assumption 1) in Section III-A, we have

$$\mathbf{R}_{\mathrm{TX}}[m] = \bar{\mathbf{R}}_{\mathrm{TX}}[m] + \tilde{\mathbf{R}}_{\mathrm{TX}}[m]. \tag{12}$$

We are interested in the structure, or more specifically the rank, of $\bar{\mathbf{R}}_{\mathrm{TX}}[m]$. To that end, we assume that $\mathbf{V}_{ab}[m] = \mathbf{v}_{\mathrm{RX},ab}[m]\mathbf{v}_{\mathrm{TX},ab}^T[m]$ and $\mathbf{\Delta}_{\phi,ab}[m] = \mathbf{d}_{\mathrm{RX},ab}[m]\mathbf{d}_{\mathrm{TX},ab}^T[m]$ with the deterministic length-N_{RX} column vectors $\mathbf{v}_{\mathrm{RX},ab}[m]$ and $\mathbf{d}_{\mathrm{RX},ab}[m]$, and the deterministic length-N_{TX} column vectors $\mathbf{v}_{\mathrm{TX},ab}[m]$ and $\mathbf{d}_{\mathrm{TX},ab}[m]$ hold.[5] In Appendix B, we show that generally $\mathrm{rank}\left\{\bar{\mathbf{R}}_{\mathrm{TX}}[m]\right\} \leq 4$ holds. In the case that only the co-polarized sub-links are affected by dominant components, we obtain $\mathrm{rank}\left\{\bar{\mathbf{R}}_{\mathrm{TX}}[m]\right\} = 2$. Finally, for an SP setup, we have $\mathrm{rank}\left\{\bar{\mathbf{R}}_{\mathrm{TX}}[m]\right\} \leq 1$. The above rank-one decompositions are only used to investigate the rank properties. In the following, we do not impose these assumptions on the TX correlation matrices.

C. Channel Decomposition

We now describe a simple method to separate the contributions of the dominant channel components and the remaining weaker scatterers from the channel correlation matrix. We thus aim at splitting $\mathbf{R}[m]$ into $\bar{\mathbf{R}}[m]$ and $\tilde{\mathbf{R}}[m]$. The method is inspired by the well-known K-factor estimation in [25], and it is simple compared to high resolution parameter estimation techniques [26]. Moreover, it is suitable for both SP and DP MIMO channels.

We use the second- and fourth-order moments of the channel $\mathbf{R}[m] = \mathrm{E}\left\{\mathbf{h}[m]\mathbf{h}^H[m]\right\}$ and $\mathbf{T}[m] = \mathrm{E}\left\{(\mathbf{h}[m]\mathbf{h}^H[m])^2\right\}$, respectively, to obtain a simple solution to the channel decomposition of $\mathbf{R}[m] = \bar{\mathbf{R}}[m] + \tilde{\mathbf{R}}[m]$ into $\bar{\mathbf{R}}[m]$ and $\tilde{\mathbf{R}}[m]$. From Appendix C, we have the relation $\mathbf{T}[m] = \mathbf{R}[m]\,\mathrm{tr}\left\{\mathbf{R}[m]\right\} + \mathbf{R}^2[m] - \bar{\mathbf{R}}^2[m]$ which can be reformulated as

$$\bar{\mathbf{R}}^2[m] = \mathbf{R}[m]\,\mathrm{tr}\left\{\mathbf{R}[m]\right\} + \mathbf{R}^2[m] - \mathbf{T}[m]. \tag{13}$$

[4]The distinction between different types of sub-links with some of them being less affected by dominant components is particularly relevant in LOS scenarios with orthogonal polarizations of matching rotation at the TX and the RX. However, we note that dominant components of the cross-polarized sub-links can also exist due to the dual-polarized radiation pattern of realistic antennas.

[5]Note that this decomposition only imposes a rank-one condition for each polarization combination, which is realistic when the distances between the TX, the RX, and possible dominant scatterers are large.

With the eigendecomposition $\bar{\mathbf{R}}[m] = \bar{\mathbf{U}}[m]\bar{\mathbf{\Lambda}}[m]\bar{\mathbf{U}}^H[m]$, we can thus directly obtain the unitary eigenvector matrix $\bar{\mathbf{U}}[m]$ and the diagonal eigenvalue matrix $\bar{\mathbf{\Lambda}}[m]$ of $\bar{\mathbf{R}}[m]$.

1) Dual-Polarized Channel: According to Section III-B1, at most four eigenvalues of $\bar{\mathbf{R}}[m]$ are non-zero; however, only two can be highly significant and smaller eigenvalues tend to be estimated less accurately. We thus have to exercise care in choosing the number of considered eigenvalues N_{DP}. Subsequently, we first find an estimate of $\bar{\mathbf{R}}[m]$ denoted as $\breve{\mathbf{R}}[m]$ according to (13). We then extract the N_{DP} largest eigenvalues of $\breve{\mathbf{R}}[m]$; this step is akin to taking the best rank-N_{DP} approximation of $\breve{\mathbf{R}}[m]$ in terms of the matrix 2-norm [27, Th. 2.5.3]. Clearly, we have $N_{\mathrm{DP}} \leq 4$. The final estimate of $\bar{\mathbf{R}}[m]$ is

$$\bar{\mathbf{R}}^{(e)}[m] = \sum_{k=1}^{N_{\mathrm{DP}}} c_k[m]\breve{\mathbf{u}}_k[m]\breve{\mathbf{u}}_k^H[m] \tag{14}$$

where the vector $\breve{\mathbf{u}}_k[m]$ denotes the eigenvector corresponding to the kth largest eigenvalue $\breve{\lambda}_k[m]$ of $\breve{\mathbf{R}}[m]$ for $k = 1, \ldots, N_{\mathrm{DP}}$. We now define the (positive semidefinite) estimates of $\mathbf{R}[m]$ and $\tilde{\mathbf{R}}[m]$ as $\mathbf{R}^{(e)}[m]$ and $\tilde{\mathbf{R}}^{(e)}[m]$, respectively. Moreover, we define $\breve{\mathbf{R}}_l[m] = \mathbf{R}^{(e)}[m] - \sum_{k=1}^{l} c_k[m]\breve{\mathbf{u}}_k[m]\breve{\mathbf{u}}_k^H[m]$ for $l = 0, \ldots, N_{\mathrm{DP}}$. The parameters $c_k[m]$ for $k = 1, \ldots, N_{\mathrm{DP}}$ are chosen such that $\tilde{\mathbf{R}}^{(e)}[m] = \mathbf{R}^{(e)}[m] - \bar{\mathbf{R}}^{(e)}[m]$ is positive semidefinite, see Appendix D:

$$c_k[m] = \begin{cases} 0, \text{ for singular } \breve{\mathbf{R}}_{k-1}[m] \\ \min\left\{\breve{\lambda}_k^+[m], \left(\breve{\mathbf{u}}_k^H[m]\breve{\mathbf{R}}_{k-1}^{-1}[m]\breve{\mathbf{u}}_k[m]\right)^{-1}\right\}, \text{else.} \end{cases} \tag{15}$$

Note that some power of the dominant components corresponding to $\breve{\mathbf{u}}_k[m]$ is transferred from $\bar{\mathbf{R}}^{(e)}[m]$ to $\tilde{\mathbf{R}}^{(e)}[m]$ whenever $c_k[m] < \breve{\lambda}_k[m]$. This might occur when the estimates of the moments $\mathbf{R}[m]$ and $\mathbf{T}[m]$ are inaccurate.

2) Single-Polarized Channel: From Section III-A, we know that $\bar{\mathbf{R}}[m]$ can at most have rank one. We thus obtain the following estimate of $\bar{\mathbf{R}}[m]$:

$$\bar{\mathbf{R}}^{(e)}[m] = c_1[m]\breve{\mathbf{u}}_1[m]\breve{\mathbf{u}}_1^H[m]. \tag{16}$$

The constant $c_1[m]$ is chosen as in (15) to ensure the positive semidefiniteness of $\tilde{\mathbf{R}}^{(e)}[m]$. We can generate SP channel realizations $\mathbf{H}^{(g)}[m]$ based on the statistical channel parameters according to

$$\mathrm{vec}\left\{\mathbf{H}^{(g)}[m]\right\} = \sqrt{c_1[m]}\ \breve{\mathbf{u}}_1[m]e^{j\phi} + \left(\tilde{\mathbf{R}}^{(e)}[m]\right)^{\frac{1}{2}}\mathbf{g} \tag{17}$$

where ϕ is uniformly distributed over $[-\pi, \pi)$, and $\mathbf{g}$ is a zero-mean proper Gaussian random column vector of length $N_{\mathrm{TX}}N_{\mathrm{RX}}$ with covariance matrix $\mathbf{I}_{N_{\mathrm{TX}}N_{\mathrm{RX}}}$; ϕ and $\mathbf{g}$ are mutually independent.

IV. Performance Assessment

With respect to the system model in Section II, the MI between the input $\mathbf{x}[m]$ and the output $\mathbf{y}[m]$ combined with instantaneous CSI at the RX is given in bit/channel use

(bit/c.u.) by

$$\begin{aligned} &I\left(\mathbf{x}[m];\mathbf{y}[m],\mathbf{H}[m]\right) \\ &= \mathrm{E}\left\{\log\det\left(\mathbf{I}_{N_{\mathrm{RX}}}+\rho\mathbf{H}[m]\mathbf{Q}[m]\mathbf{H}^H[m]\right)\right\} \\ &\overset{(a)}{=} \mathrm{E}\left\{\log\det\left(\mathbf{I}_{N_{\mathrm{TX}}}+\rho\mathbf{H}^H[m]\mathbf{H}[m]\mathbf{Q}[m]\right)\right\} \end{aligned} \tag{18}$$

where the expectation is taken over $\mathbf{H}[m]$ and, in (a), we used [28, Th. 1.3.20]. Note that the MI in (18) is time-dependent as the channel is in general non-stationary, i.e., the expectation over the channel yields a statistical parameter that changes over time. Therefore, in a strict sense, (18) is not an achievable rate. Nevertheless, we use the MI (18) as performance measure since it has an interpretation in terms of an achievable rate in bit/channel use (bit/c.u.) for non-stationary slow- and fast-fading wireless channels [29], [30].

With Appendix E, we can state the following second-order approximation of (18):

$$\begin{aligned} &I\left(\mathbf{x}[m];\mathbf{y}[m],\mathbf{H}[m]\right) \\ &\approx I^{(\mathrm{a})}\left(\rho,\mathbf{Q}[m],\mathbf{R}_{\mathrm{TX}}[m],\mathbf{Z}[m]\right) \\ &= \log\det\left(\mathbf{I}_{N_{\mathrm{TX}}}+\rho\mathbf{R}_{\mathrm{TX}}^{*}[m]\mathbf{Q}[m]\right)-\frac{\log(e)\rho^2}{2} \\ &\quad\times\mathrm{tr}\left\{\mathbf{Z}[m]\left(\left(\mathbf{Q}[m]\left(\mathbf{I}_{N_{\mathrm{TX}}}+\rho\mathbf{R}_{\mathrm{TX}}^{*}[m]\mathbf{Q}[m]\right)^{-1}\right)^{T}\right.\right. \\ &\quad\left.\left.\otimes\left(\mathbf{Q}[m]\left(\mathbf{I}_{N_{\mathrm{TX}}}+\rho\mathbf{R}_{\mathrm{TX}}^{*}[m]\mathbf{Q}[m]\right)^{-1}\right)\right)\right\} \end{aligned} \tag{19}$$

with the $N_{\mathrm{TX}}^2\times N_{\mathrm{TX}}^2$ fourth-order moment matrix of the channel

$$\begin{aligned} \mathbf{Z}[m]=\mathrm{E}\Big\{&\mathrm{vec}\left\{\mathbf{H}^H[m]\mathbf{H}[m]-\mathbf{R}_{\mathrm{TX}}^{*}[m]\right\} \\ &\left(\mathrm{vec}\left\{\mathbf{H}^H[m]\mathbf{H}[m]-\mathbf{R}_{\mathrm{TX}}^{*}[m]\right\}\right)^H\Big\}. \end{aligned} \tag{20}$$

Additionally to $\mathbf{R}_{\mathrm{TX}}[m]$, (19) requires the evaluation of the fourth-order moment of the channel $\mathbf{Z}[m]$. In order to gain insight on the influence of typical statistical channel parameters on the MI, we rewrite $\mathbf{Z}[m]$ as a function of $\bar{\mathbf{R}}[m]$ and $\tilde{\mathbf{R}}[m]$ only. Both of these parameters are available with the channel decomposition in Section III-C. In order to restate (20) for SP as well as for DP channels, we assume that only the co-polarized sub-links can be affected by dominant components. In Appendix F, we then obtain the following result:

$$\begin{aligned} \mathrm{vec}\left\{\mathbf{Z}[m]\right\} &= \left(\mathbf{I}_{N_{\mathrm{TX}}}\otimes\mathbf{Y}[m]\right)\mathrm{vec}\left\{\mathbf{R}[m]\right\} \\ &\quad+\left(\mathbf{K}_{N_{\mathrm{TX}},N_{\mathrm{TX}}}\otimes\mathbf{K}_{N_{\mathrm{TX}},N_{\mathrm{TX}}}\right) \\ &\quad\times\left(\mathbf{I}_{N_{\mathrm{TX}}}\otimes\mathbf{Y}^{*}[m]\right)\mathrm{vec}\left\{\bar{\mathbf{R}}^{*}[m]\right\} \end{aligned} \tag{21}$$

with the $N_{\mathrm{TX}}^3\times N_{\mathrm{TX}}N_{\mathrm{RX}}^2$ block matrix $\mathbf{Y}[m]$ containing $\mathbf{I}_{N_{\mathrm{TX}}}\otimes\mathbf{X}_{k,l}[m]$ in the kth row-partition and the lth column-partition for $k=1,\ldots,N_{\mathrm{TX}}$ and $l=1,\ldots,N_{\mathrm{RX}}$. The $N_{\mathrm{TX}}\times N_{\mathrm{RX}}$ matrix $\mathbf{X}_{k,l}[m]$ is defined by $\left[\mathbf{X}_{k,l}[m]\right]_{p,q}=\left[\tilde{\mathbf{R}}[m]\right]_{(k-1)N_{\mathrm{RX}}+l,(p-1)N_{\mathrm{RX}}+q}$ for $p=1,\ldots,N_{\mathrm{TX}}$ and $q=1,\ldots,N_{\mathrm{RX}}$. Note that $\mathbf{R}[m]=\bar{\mathbf{R}}[m]+\tilde{\mathbf{R}}[m]$ holds.

A. SP vs. DP Performance: High-K-Factor Case

We now compare the performance of SP and DP setups in the high-K-factor regime. First, consider the case of an asymptotic K-factor setting, i.e., infinitely large K-factors, and that only the co-polarized sub-links have dominant components. Then, the Jensen bound on the MI given by

$$\begin{aligned} &I^{(\mathrm{J})}\left(\rho,\mathbf{Q}[m],\mathbf{R}_{\mathrm{TX}}[m]\right) \\ &= \log\det\left(\mathbf{I}_{N_{\mathrm{TX}}}+\rho\mathbf{R}_{\mathrm{TX}}^{*}[m]\mathbf{Q}[m]\right) \end{aligned} \tag{22}$$

and corresponding to the first term in (19) is equal to the MI (18); it can thus be used for a simple analytical performance evaluation. Note that the channel influences the Jensen bound on the MI, i.e., (22), only through $\mathbf{R}_{\mathrm{TX}}[m]$. In the asymptotic K-factor setting, we have $\mathbf{R}_{\mathrm{TX}}[m]=\bar{\mathbf{R}}_{\mathrm{TX}}[m]$.

Using Hadamard's inequality [28, Sec. 7.8.1], it can be shown that (22) is maximized by choosing the eigenvectors of the input covariance matrix $\mathbf{Q}[m]$ to be given by the eigenvectors of $\mathbf{R}_{\mathrm{TX}}^{*}[m]$. I.e., for the eigendecomposition $\mathbf{R}_{\mathrm{TX}}^{*}[m]=\mathbf{U}_{\mathrm{TX}}[m]\mathbf{\Lambda}_{\mathrm{TX}}[m]\mathbf{U}_{\mathrm{TX}}^H[m]$ with the unitary eigenvector matrix $\mathbf{U}_{\mathrm{TX}}[m]$ and the diagonal eigenvalue matrix $\mathbf{\Lambda}_{\mathrm{TX}}[m]$ of $\mathbf{R}_{\mathrm{TX}}^{*}[m]$, we obtain $\mathbf{Q}[m]=\mathbf{U}_{\mathrm{TX}}[m]\mathbf{\Lambda}_{Q}[m]\mathbf{U}_{\mathrm{TX}}^H[m]$. Here, $\mathbf{\Lambda}_{Q}[m]$ is the diagonal eigenvalue matrix of $\mathbf{Q}[m]$ determining the power allocation. Furthermore, we define $\lambda_{\mathrm{TX},k}[m]=[\mathbf{\Lambda}_{\mathrm{TX}}[m]]_{k,k}$ and $\lambda_{Q,k}[m]=[\mathbf{\Lambda}_{Q}[m]]_{k,k}$ for $k=1,\ldots,N_{\mathrm{TX}}$, where $\lambda_{\mathrm{TX},k}[m]\geq\lambda_{\mathrm{TX},k+1}[m]$ for $k=1,\ldots,N_{\mathrm{TX}}-1$ holds.

The crossing points between the MI of an SP setup and the MI of a DP setup are then given by

$$\begin{aligned} &I^{(\mathrm{J})}\left(\rho,\mathbf{Q}_{\mathrm{TX,SP}}[m],\mathbf{R}_{\mathrm{TX,SP}}[m]\right) \\ &= I^{(\mathrm{J})}\left(\rho,\mathbf{Q}_{\mathrm{TX,DP}}[m],\mathbf{R}_{\mathrm{TX,DP}}[m]\right) \end{aligned} \tag{23}$$

which is equivalent to

$$\begin{aligned} &\log\left(\prod_{k=1}^{N_{\mathrm{TX}}}\left(1+\rho\lambda_{\mathrm{TX,SP},k}[m]\lambda_{Q,\mathrm{SP},k}[m]\right)\right) \\ &= \log\left(\prod_{k=1}^{N_{\mathrm{TX}}}\left(1+\rho\lambda_{\mathrm{TX,DP},k}[m]\lambda_{Q,\mathrm{DP},k}[m]\right)\right) \end{aligned} \tag{24}$$

where $\lambda_{\mathrm{TX,SP},k}[m]$ and $\lambda_{\mathrm{TX,DP},k}[m]$ for $k=1,\ldots,N_{\mathrm{TX}}$ are the eigenvalues of the SP and DP transmit correlation matrices $\mathbf{R}_{\mathrm{TX,SP}}[m]$ and $\mathbf{R}_{\mathrm{TX,DP}}[m]$, respectively. Similarly, $\lambda_{Q,\mathrm{SP},k}[m]$ and $\lambda_{Q,\mathrm{DP},k}[m]$ for $k=1,\ldots,N_{\mathrm{TX}}$ are the eigenvalues of the SP and the DP input covariance matrices $\mathbf{Q}_{\mathrm{TX,SP}}[m]$ and $\mathbf{Q}_{\mathrm{TX,DP}}[m]$, respectively. As highlighted in Section III-B2, we have $\mathrm{rank}\left\{\bar{\mathbf{R}}_{\mathrm{TX}}[m]\right\}=2$ if only the co-polarized sub-links have dominant components and we have $\mathrm{rank}\left\{\bar{\mathbf{R}}_{\mathrm{TX}}[m]\right\}=1$ in the SP case with a dominant component. In the high-K-factor regime with dominant components for co-polarized propagation only, we thus have to decide between an SP setup with one transmitted stream and a DP setup with two transmitted streams.

To obtain the crossing points when $\lambda_{\mathrm{TX,SP},1}[m]>0$, $\lambda_{\mathrm{TX,DP},k}[m]>0$, and $\lambda_{Q,\mathrm{DP},k}[m]>0$ for $k=1,2$, we simplify (24) to

$$\begin{aligned} &\log\left(1+\rho\lambda_{\mathrm{TX,SP},1}[m]\right) \\ &= \log\left(\prod_{k=1}^{2}\left(1+\rho\lambda_{\mathrm{TX,DP},k}[m]\lambda_{Q,\mathrm{DP},k}[m]\right)\right) \end{aligned} \tag{25}$$

or equivalently

$$1+\rho\lambda_{\mathrm{TX,SP},1}[m]=\prod_{k=1}^{2}\left(1+\rho\lambda_{\mathrm{TX,DP},k}[m]\lambda_{Q,\mathrm{DP},k}[m]\right). \tag{26}$$

Besides the crossing point at $\rho = 0$, there is a crossing point at

$$\rho_{\text{CP}}^{(\text{J})}[m] = \frac{\lambda_{\text{TX,SP},1}[m] - \lambda_{\text{sum,DP}}[m]}{\lambda_{\text{prod,DP}}[m]} \tag{27}$$

which is positive if $\lambda_{\text{TX,SP},1}[m] > \lambda_{\text{sum,DP}}[m]$. Here, we defined

$$\begin{aligned}&\lambda_{\text{sum,DP}}[m]\\ &= \lambda_{\text{TX,DP},1}[m]\lambda_{Q,\text{DP},1}[m] + \lambda_{\text{TX,DP},2}[m]\lambda_{Q,\text{DP},2}[m] \qquad (28)\\ &\lambda_{\text{prod,DP}}[m]\\ &= \lambda_{\text{TX,DP},1}[m]\lambda_{Q,\text{DP},1}[m]\lambda_{\text{TX,DP},2}[m]\lambda_{Q,\text{DP},2}[m]. \qquad (29)\end{aligned}$$

By inspecting (26), we observe that the contribution of the MI of the SP setup, i.e., the left hand side of (26), is a linear function of the SNR ρ, while the contribution of the MI of the DP setup, i.e., the right hand side of (26), grows quadratically with the SNR ρ. We thus conclude the following: If $\lambda_{\text{TX,SP},1}[m] > \lambda_{\text{sum,DP}}[m]$ holds, then the DP setup outperforms the SP setup in terms of MI only at SNR values above $\rho_{\text{CP}}^{(\text{J})}[m]$. If $\lambda_{\text{TX,SP},1}[m] \leq \lambda_{\text{sum,DP}}[m]$ holds, the DP setup always matches or exceeds the MI of the SP setup. We note that these results can be exploited based on only statistical knowledge of the channel.

B. SP vs. DP Performance: General Case

In this section, we study the performance of the SP and the DP setup in the general case of arbitrary K-factors. Now, we need to consider the approximate evaluation of the MI (19) and cannot restrict to the Jensen bound on the MI. Similarly to Section IV-A, we consider the case of the SP setup transmitting a single stream and the DP setup transmitting two streams with positive $\lambda_{\text{TX,SP},1}[m]$, $\lambda_{\text{TX,DP},k}[m]$, and $\lambda_{Q,\text{DP},k}[m]$ for $k = 1, 2$. Furthermore, we again choose the eigenvectors of $\mathbf{R}_{\text{TX}}^{*}[m]$ as the eigenvectors of the input covariance matrix $\mathbf{Q}[m]$. In order to get a closed-form expression of the crossing points, we derive a lower bound on the approximate MI (19) in Appendix G. It is given by

$$\begin{aligned}&I^{(\text{LB})}\left(\rho, \mathbf{Q}[m], \mathbf{R}_{\text{TX}}[m], \mathbf{Z}[m]\right)\\ &= \log\det\left(\mathbf{I}_{N_{\text{TX}}} + \rho\mathbf{R}_{\text{TX}}^{*}[m]\mathbf{Q}[m]\right) - \log(e)w[m] \qquad (30)\end{aligned}$$

with

$$w[m] = \sum_{k=1}^{N_{\text{st}}}\sum_{l=1}^{N_{\text{st}}} \frac{\left[\mathbf{Z}^{(U)}[m]\right]_{(k-1)N_{\text{TX}}+l,(k-1)N_{\text{TX}}+l}}{2\lambda_{\text{TX},k}[m]\lambda_{\text{TX},l}[m]} \tag{31}$$

$$\mathbf{Z}^{(U)}[m] = \left(\mathbf{U}_{\text{TX}}^{T}[m] \otimes \mathbf{U}_{\text{TX}}^{H}[m]\right)\mathbf{Z}[m]\left(\mathbf{U}_{\text{TX}}^{*}[m] \otimes \mathbf{U}_{\text{TX}}[m]\right) \tag{32}$$

and the number of transmitted streams N_{st}. We note that this lower bound is tight in the limit $\rho \to \infty$. Based on (30), we calculate the crossing points of the MI of the SP setup and the MI of the DP setup by considering

$$\begin{aligned}&I^{(\text{LB})}\left(\rho, \mathbf{Q}_{\text{TX,SP}}[m], \mathbf{R}_{\text{TX,SP}}[m], \mathbf{Z}_{\text{SP}}[m]\right)\\ &= I^{(\text{LB})}\left(\rho, \mathbf{Q}_{\text{TX,DP}}[m], \mathbf{R}_{\text{TX,DP}}[m], \mathbf{Z}_{\text{DP}}[m]\right) \qquad (33)\end{aligned}$$

where $\mathbf{Z}_{\text{SP}}[m]$ and $\mathbf{Z}_{\text{DP}}[m]$ denote the matrix $\mathbf{Z}[m]$ for the SP and the DP case, respectively. Similar to Section IV-A, we note the linear and the quadratic growth with the SNR ρ of the exponentiation (with respect to the base 2) of the MI (30) for the SP and the DP setup, respectively. We then obtain a crossing point above which the DP setup outperforms the SP setup in terms of MI at

$$\begin{aligned}\rho_{\text{CP}}^{(\text{LB})}[m] &= \frac{\lambda_{\text{TX,SP},1}[m]\alpha[m] - \lambda_{\text{sum,DP}}[m]}{2\lambda_{\text{prod,DP}}[m]}\\ &+\sqrt{\left(\frac{\lambda_{\text{TX,SP},1}[m]\alpha[m] - \lambda_{\text{sum,DP}}[m]}{2\lambda_{\text{prod,DP}}[m]}\right)^2 + \frac{\alpha[m]-1}{\lambda_{\text{prod,DP}}[m]}} \qquad (34)\end{aligned}$$

if the condition $4(1-\alpha[m])\lambda_{\text{prod,DP}}[m] \leq (\lambda_{\text{TX,SP},1}[m]\alpha[m] - \lambda_{\text{sum,DP}}[m])^2$ holds. If this condition does not hold, the DP setup always outperforms the SP setup. Here, we defined $\alpha[m] = \exp(w_{\text{DP}}[m] - w_{\text{SP}}[m])$, which is a correction factor, and $w_{\text{SP}}[m]$ and $w_{\text{DP}}[m]$ are obtained from (31) for the SP and the DP case, respectively. When $\alpha[m] = 1$, we recover the solution (27).

V. Channel Measurements

We evaluate the previously obtained results using urban macrocell channel measurements that were performed at 2.53 GHz in two bands of 45 MHz in Ilmenau, Germany. During the measurement campaign, the DP MIMO channel from three base station (BS) positions with different heights to a multitude of MT tracks was measured sequentially. The MT was moving with a maximal velocity of about 10 km/h. In this paper, we extract the 20 MHz band centered at 2.505 GHz, and we use the three BS positions at a height of 25 m with the three MT reference tracks. For further details regarding the measurement campaign, see [31], [32].

After denoising the channel measurements in the time-delay domain, we normalize the channel matrices $\mathbf{H}[m]$. The normalization is performed with a scalar factor such that $\text{E}\left\{||\mathbf{h}_{\text{co}}[m]||_F^2\right\} = N_{\text{co}}$ is emulated inside each stationarity region containing $N_t = 16$ samples in time and $N_f = 128$ samples in frequency. Here, $\mathbf{h}_{\text{co}}[m]$ is a vector containing only the N_{co} elements of $\mathbf{H}[m]$ corresponding to co-polarized sub-links. This guarantees a fair comparison between SP and DP setups since we account for the power loss in cross-polarized sub-links. Then, we estimate the statistical quantities by replacing the ensemble averaging with an averaging over N_t time and N_f frequency samples. This yields a total of 2048 (≈ 500 non-coherent) realizations [32].

A. Antenna Setups

We choose a uniform linear array at the BS and two uniform circular arrays (UCAs), which lie on top of each other, at the MT for the subsequent evaluations. The antenna arrays consist of patch antennas that can be excited vertically and horizontally. Due to the UCAs at the MT, we are able to differentiate between the following four orientations: the front (direction of motion), the back, and the two sides of the MT. For our evaluations, the BS and the MT act as the TX and the RX, respectively. We consider two SP antenna setups, a VP and an HP setup, as well as two DP antenna setups, a co-located (DP-CL) and a spatially separated (DP-SS) setup,

TABLE I
SPECIFICATION AND PROPERTIES OF THE REFERENCE LINKS

Link	BS	Track	MT orient.	MT pos. [m]	K-Factors
1	1	41a-42	back	$0-34.9$	low
2	3	9a-9b	left	$0-38.9$	medium
3	2	10b-9a	front	$9.8-56.8$	high
4	3	10b-9a	left	$0-64.9$	varying

for the 4×4 MIMO case. For the SP setups, the antennas are separated by λ_c at the TX and $0.5\lambda_c$ (different UCAs) or $0.327\lambda_c$ (same UCA) at the RX. For the co-located DP-CL setup, the antenna patches at the TX and the RX are separated by $3\lambda_c$ and $0.5\lambda_c$ (across the UCAs), respectively. For the spatially separated DP-SS setup, we use the same antenna patches as in the SP case. However, we have a separation of $2\lambda_c$ between antennas of the same polarization at the TX side. At the RX side, the lower UCA is only used for the VP excitation while the upper UCA is only used for the HP excitation. We note that all setups result in the same array length at the TX.

B. Scenario Classification

Based on the measurements, for the SP case, we mainly observe links with either low K-factors and low correlations between the MIMO sub-links or links with high K-factors and high correlations. A similar observation was made in [33] and [34]. Thus, similar to [34], we classify the measurements into links with low, medium, and high (co-polarized) K-factors, see Table I. The low K-factor links are characterized by K-factor values in $[0, 2]$, while the medium and high K-factors links have several peaks with values above 5 and 10, respectively. Additionally, we have one link with varying K-factors which consists of low and high K-factor parts. The reason for the low K-factors/correlations in link 1 and 2 is that track 41a-42 is partly located in a street canyon; regarding BS 1 and 3 no dominant components are expected. In contrast, tracks 9a-9b and 10b-9a are mostly situated in an open environment where dominant components are more likely to occur.

VI. RESULTS

In order to check the efficiency of the channel decomposition, we compare the K-factors from the decomposition to the ones obtained from the measurements with the moment method in [25]. The results on the K-factors are averaged over the sub-links of each polarization combination for the DP-CL setup. Subsequently, we consider the practically relevant case of extracting $N_{\text{DP}} = 2$ eigenvalues, see Section III-C1. First, we use synthetic data generated using the 4×4 DP channel model introduced in [1]. We adapt the channel model to our antenna setups and the mobile scenario by allowing for individual K-factors of the sub-links and setting the same phases for the dominant components of the same polarization combination, while the phases are independent for different polarization combinations. The cross-polarized sub-links do not experience any dominant components. We use the parameters $\alpha = \alpha_f = 0.1$, $r_s = t_s = 0.7$, and $r_p = t_p = 0.2$ and a common K-factor for the co-polarized sub-links. For the estimation of the K-factors, we mimic the averaging lengths of the measurement-based case. The results averaged over 200 realizations are given in Table II for different K-factors (all in linear scale). We can see that both the moment method and our channel decomposition yield accurate values. In Table III, we show the results (in linear scale) for the links 1-3 averaged over the driven distance. We see that the cross-polarized sub-links, VP to HP (V-H) and HP to VP (H-V), show significantly smaller K-factors than the co-polarized ones, VP to VP (V-V) and HP to HP (H-H). In general, we observe lower K-factor values from the channel decomposition; this is due to guaranteeing the positive semidefiniteness of the correlation matrices, which can result in a shift of the power from the dominant components to the remaining components of the channel, see Section III-C. In Fig. 1, we depict the evolution of the K-factors (in linear scale) over distance for link 4 since it is characterized by varying K-factors, see Table I. Similar observations as in Table III can be made. Furthermore, we observe that the channel decomposition is able to reproduce the tendencies in the evolution of the measured K-factors.

TABLE II
AVERAGE K-FACTORS FROM THE SIMULATED CHANNEL AND THE PROPOSED CHANNEL DECOMPOSITION

Co-pol.	K-factors: Simulation				K-factors: Decomposition			
K-factor	V-V	H-H	V-H	H-V	V-V	H-H	V-H	H-V
1	1.0	1.0	0.1	0.1	1.0	1.0	0.0	0.0
5	5.0	5.0	0.1	0.1	5.0	5.0	0.0	0.0
10	10.0	10.0	0.1	0.1	10.1	10.0	0.0	0.0

TABLE III
AVERAGE K-FACTORS FROM THE MEASURED CHANNEL AND THE PROPOSED CHANNEL DECOMPOSITION

	K-factors: Measurements				K-factors: Decomposition			
Link	V-V	H-H	V-H	H-V	V-V	H-H	V-H	H-V
1	0.5	0.8	0.4	0.4	0.5	0.6	0.3	0.3
2	1.6	1.4	0.6	0.7	1.2	0.9	0.2	0.2
3	4.0	5.7	1.9	1.8	4.0	5.4	1.7	1.5

We now review some results of the comparison of SP and DP MIMO systems from the literature. However, we note that previous results often rely on different assumptions regarding the CSI and the used performance measure. Nevertheless, we gather the main findings. Unless otherwise mentioned, the cited works assume that the TX has no CSI and they evaluate the performance in terms of the instantaneous MI. We assume the existence of statistical CSI at the TX, and we use the ergodic MI which is also a suitable performance measure in fast fading scenarios. In [11], indoor measurements at 2.4 GHz reveal that SP mostly outperform DP setups for 2×2 and 4×4 MIMO systems at an SNR of 20 dB, especially for low K-factors. However, in [12] indoor measurements at 1.95 GHz show that DP should be favored over SP 4×4 MIMO systems at an SNR of 20 dB. Outdoor measurements at 2.5 GHz in [13] favor a DP over an SP TX setup with a DP RX setup in both cases, but at an SNR of 10 dB and for 2×3 MIMO systems. In [35], the throughput of 2×2 and 4×4

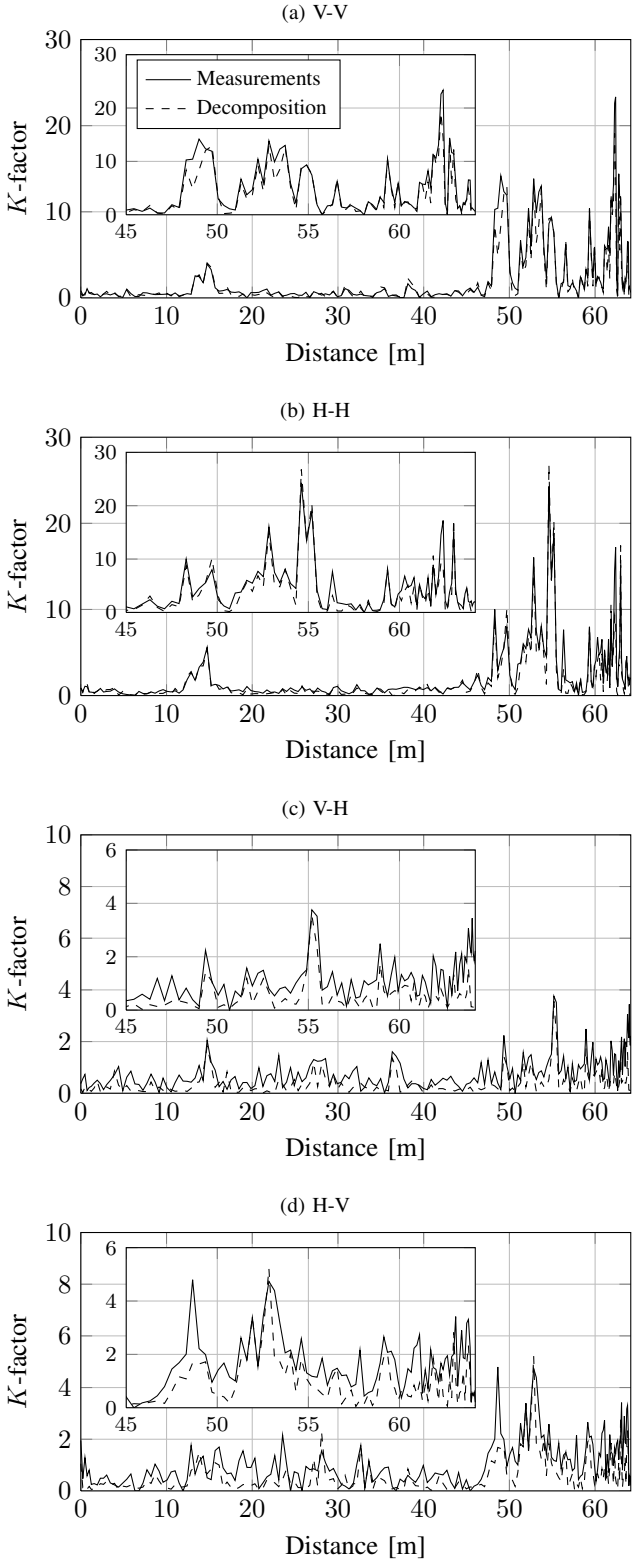

Fig. 1. K-factors vs. distance on link 4 (averaged over sub-links of the DP-CL setup with the same polarization combination).

MIMO systems is investigated in an LTE setting with the same measurements as in this work. It is found that DP outperform SP setups, for closed-loop spatial multiplexing, above certain SNR thresholds. In [1], simulations for 2×2 MIMO systems are used to evaluate the benefits of DP vs. SP setups in terms of the ergodic MI for SNRs between 0 and 20 dB. The results show that there is a cross-polarization discrimination threshold above which SP outperform DP setups, and there is a K-factor threshold above which DP outperform SP setups for SNRs around 10 dB.

Next, we evaluate the performance of the SP and the DP setups. In order to compare the approximate evaluation of the MI, i.e., (19) with (21), to the (exact) MI (18), we use $N_{\text{DP}} = 2$. We use the optimal input with respect to the Jensen bound on the MI, where the eigenvectors of $\mathbf{R}_{\text{TX}}^{*}[m]$ form the precoding and the power allocation is obtained by a simple water-filling strategy [36], unless otherwise specified. The results of links 1-3 are accumulated over each track and shown as a function of the SNR in Fig. 2. We observe that only at high SNRs there is a noticeable gap between the MI and its approximate evaluation. The DP-CL setup only provides an advantage in terms of the MI compared to the SP setups, i.e., the VP and the HP setup, if the K-factors (of the co-polarized sub-links) and the SNR attain certain values; the higher the K-factors, the lower this SNR threshold is. Practically, a switching between SP and DP setups is thus most useful in medium- to high-K-factor scenarios; there the crossing points between the MI of the SP setups and the DP-CL setup are accurately reproduced by the approximate evaluation of the MI, i.e., (19) with (21). Furthermore, in Fig. 3, we plot the MI over distance for the VP, the HP, and the DP-CL setup on link 4 at an SNR of 10 dB. We observe that the positions at which the DP-CL setup outperforms the SP setups coincide with high K-factors, see Fig. 1.

We now compare the performance using two different DP setups, the DP-CL setup with co-located antennas and the DP-SS setup with spatially separated antennas. In Fig. 4, we show the MI of the DP-CL and the DP-SS setup, exemplarily, on link 2. We observe that the DP-SS setup is able to reach even higher MI values at high SNR. We expect that this is due to the increased viewing angle into the propagation channel for each polarization at the RX side, which results in an increase in the degrees of freedom. The DP-CL setup, however, offers a more compact antenna array at the cost of a reduced viewing angle at the RX. Furthermore, we observe here that the approximate evaluation of the MI is more accurate for the DP-SS setup than it is for the DP-CL setup.

The average SNR values above which the MI of the DP-CL setup with two streams and equal power allocation is higher than the MI of the VP or the HP setup with a single stream are given Table IV. Note that the precoding is again given by the eigenvectors of $\mathbf{R}_{\text{TX}}^{*}[m]$. The resulting crossing points are calculated using the various methods introduced before, i.e., using the MI and the approximations given in (18), (19), (22), and (30) together with (21). We observe that the approximate evaluation of the MI (19) is able to accurately reproduce the average SNR values. When using the Jensen bound on the MI, we obtain lower average SNR values. Note that the Jensen bound on the MI is only useful for high-K-factor links; thus, we only give the results for link 3. The SNR values obtained from the lower bound on the approximate MI, i.e., (30), yield a slight overestimation of the average SNR values for all links.

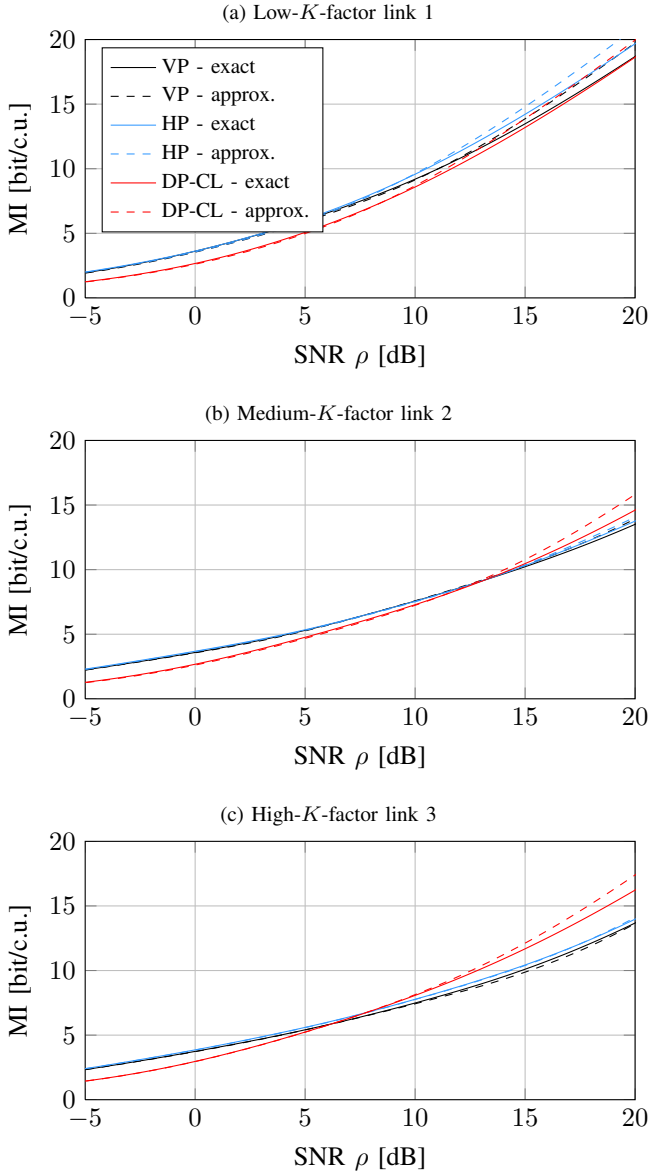

Fig. 2. MI vs. SNR of the exact and the approximate evaluation for the VP, the HP, and the DP-CL setup.

We observe that all the (exact) crossing points are roughly between 5 and 7 dB. A clear dependence on the link is not present; this is due to the restriction to two transmitted streams for DP MIMO systems and one transmitted stream for SP MIMO systems.

VII. Conclusion

In this paper, we have studied the modeling of DP MIMO channels as well as the performance over such channels. We proposed a general model for DP mobile Ricean channels with a channel decomposition technique yielding necessary statistical channel parameters. Furthermore, we derived an approximation of the MI, which is a function of those parameters, in order to gain some understanding on the statistical channel parameters influencing the MI. Based on the approximate evaluation of the MI, we were able to analytically characterize

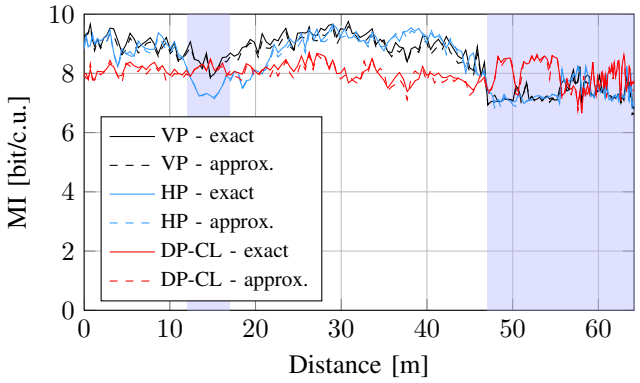

Fig. 3. MI vs. distance for the exact and the approximate evaluation for the VP, the HP, and the DP-CL setup on link 4 with an SNR $\rho = 10$ dB (the blue-shaded regions denote positions where the (co-polarized) K-factors are high, cf. Fig. 1).

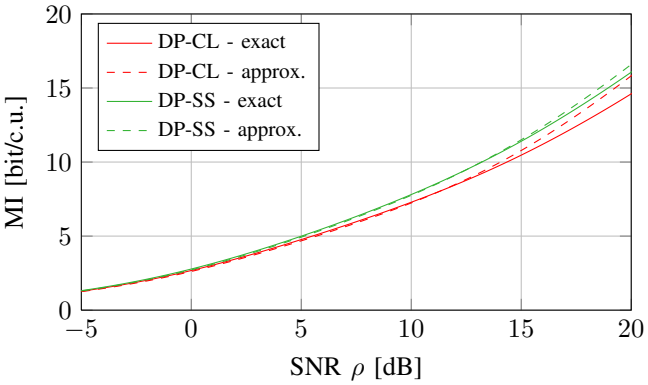

Fig. 4. MI vs. SNR for the DP-CL and the DP-SS setup on link 2.

TABLE IV
Average SNR Values Above Which the MI of the DP-CL Setup with Two Streams and Equal Power Allocation is Higher than the MI of an SP Setup with a Single Stream

	SNR Values ρ_{CP} [dB] (averaged)					
	VP vs. DP-CL			HP vs. DP-CL		
Method	**Link 1**	**Link 2**	**Link 3**	**Link 1**	**Link 2**	**Link 3**
Exact: (18)	4.998	6.759	5.242	5.559	7.197	5.744
Appr.: (19)	5.073	7.027	5.240	5.567	7.324	5.680
$\rho_{\mathrm{CP}}^{(\mathrm{J})}$: (22)	—	—	4.623	—	—	4.813
$\rho_{\mathrm{CP}}^{(\mathrm{LB})}$: (30)	6.154	7.722	5.747	6.564	7.976	6.130

the required SNR for a dual-stream DP MIMO system to outperform a single-stream SP MIMO system. Finally, we applied the obtained results to channel measurements performed in an urban macrocell environment at 2.53 GHz. We find that for sufficiently high K-factors DP MIMO systems are able to outperform SP MIMO systems if a certain, practically relevant, SNR is attained.

Appendix A
Rank of $\bar{\mathbf{R}}[m]$

We are interested in a condition on the rank of $\bar{\mathbf{R}}[m]$ for the DP case. We first drop the time argument for notational

simplicity. Then, we rearrange $\bar{\mathbf{R}}$ through column and row permutations with the permutation matrix $\mathbf{P}$ into $\bar{\mathbf{R}}^{(\mathrm{p})} = \mathbf{P}\bar{\mathbf{R}}\mathbf{P}^T$ such that

$$\bar{\mathbf{R}}^{(\mathrm{p})} = \begin{bmatrix} \bar{\mathbf{R}}_{\mathrm{VVVV}} & \bar{\mathbf{R}}_{\mathrm{VVVH}} & \bar{\mathbf{R}}_{\mathrm{VVHV}} & \bar{\mathbf{R}}_{\mathrm{VVHH}} \\ \bar{\mathbf{R}}_{\mathrm{VHVV}} & \bar{\mathbf{R}}_{\mathrm{VHVH}} & \bar{\mathbf{R}}_{\mathrm{VHHV}} & \bar{\mathbf{R}}_{\mathrm{VHHH}} \\ \bar{\mathbf{R}}_{\mathrm{HVVV}} & \bar{\mathbf{R}}_{\mathrm{HVVH}} & \bar{\mathbf{R}}_{\mathrm{HVHV}} & \bar{\mathbf{R}}_{\mathrm{HVHH}} \\ \bar{\mathbf{R}}_{\mathrm{HHVV}} & \bar{\mathbf{R}}_{\mathrm{HHVH}} & \bar{\mathbf{R}}_{\mathrm{HHHV}} & \bar{\mathbf{R}}_{\mathrm{HHHH}} \end{bmatrix} \tag{35}$$

with $\bar{\mathbf{R}}_{abcd} = \mathrm{E}\left\{\mathrm{vec}\left\{\bar{\mathbf{H}}_{ab}\right\}\left(\mathrm{vec}\left\{\bar{\mathbf{H}}_{cd}\right\}\right)^H\right\}$ for $a,b,c,d \in \{\mathrm{V},\mathrm{H}\}$ holds. We now have

$$\begin{aligned}\bar{\mathbf{R}}^{(\mathrm{p})} &\overset{(a)}{=} \left(\mathrm{vec}\left\{\mathbf{V}\right\}\left(\mathrm{vec}\left\{\mathbf{V}\right\}\right)^H\right) \odot \mathrm{E}\left\{\mathrm{vec}\left\{\boldsymbol{\Phi}\right\}\left(\mathrm{vec}\left\{\boldsymbol{\Phi}\right\}\right)^H\right\} \\ &\overset{(b)}{=} \left(\mathrm{vec}\left\{\mathbf{V}\right\}\left(\mathrm{vec}\left\{\mathbf{V}\right\}\right)^H\right) \\ &\quad \odot \left(\mathrm{vec}\left\{\boldsymbol{\Delta}_\phi\right\}\left(\mathrm{vec}\left\{\boldsymbol{\Delta}_\phi\right\}\right)^H\right) \\ &\quad \odot \left(\mathbf{G} \otimes \mathbf{1}_{\frac{N_{\mathrm{TX}}N_{\mathrm{RX}}}{4}}\right)\end{aligned} \tag{36}$$

where, in (a), we used (3) and defined

$$\begin{aligned}\mathrm{vec}\left\{\mathbf{V}\right\} = \Big[&\left(\mathrm{vec}\left\{\mathbf{V}_{\mathrm{VV}}\right\}\right)^T \left(\mathrm{vec}\left\{\mathbf{V}_{\mathrm{VH}}\right\}\right)^T \\ &\left(\mathrm{vec}\left\{\mathbf{V}_{\mathrm{HV}}\right\}\right)^T \left(\mathrm{vec}\left\{\mathbf{V}_{\mathrm{HH}}\right\}\right)^T\Big]^T\end{aligned} \tag{37}$$

$$\begin{aligned}\mathrm{vec}\left\{\boldsymbol{\Phi}\right\} = \Big[&\left(\mathrm{vec}\left\{\boldsymbol{\Phi}_{\mathrm{VV}}\right\}\right)^T \left(\mathrm{vec}\left\{\boldsymbol{\Phi}_{\mathrm{VH}}\right\}\right)^T \\ &\left(\mathrm{vec}\left\{\boldsymbol{\Phi}_{\mathrm{HV}}\right\}\right)^T \left(\mathrm{vec}\left\{\boldsymbol{\Phi}_{\mathrm{HH}}\right\}\right)^T\Big]^T\end{aligned} \tag{38}$$

and, in (b), we used (4) and defined

$$\begin{aligned}\mathrm{vec}\left\{\boldsymbol{\Delta}_\phi\right\} = \Big[&\left(\mathrm{vec}\left\{\boldsymbol{\Delta}_{\phi,\mathrm{VV}}\right\}\right)^T \left(\mathrm{vec}\left\{\boldsymbol{\Delta}_{\phi,\mathrm{VH}}\right\}\right)^T \\ &\left(\mathrm{vec}\left\{\boldsymbol{\Delta}_{\phi,\mathrm{HV}}\right\}\right)^T \left(\mathrm{vec}\left\{\boldsymbol{\Delta}_{\phi,\mathrm{HH}}\right\}\right)^T\Big]^T\end{aligned} \tag{39}$$

$$\mathbf{G} = \begin{bmatrix} 1 & g_{\mathrm{VVVH}} & g_{\mathrm{VVHV}} & g_{\mathrm{VVHH}} \\ g_{\mathrm{VHVV}} & 1 & g_{\mathrm{VHHV}} & g_{\mathrm{VHHH}} \\ g_{\mathrm{HVVV}} & g_{\mathrm{HVVH}} & 1 & g_{\mathrm{HVHH}} \\ g_{\mathrm{HHVV}} & g_{\mathrm{HHVH}} & g_{\mathrm{HHHV}} & 1 \end{bmatrix} \tag{40}$$

with $g_{abcd} = \mathrm{E}\left\{e^{j(\phi_{ab}-\phi_{cd})}\right\}$ for $a,b,c,d \in \{\mathrm{V},\mathrm{H}\}$ and the all-one matrix $\mathbf{1}_N$ of size $N \times N$. As the rank of a matrix is unchanged by left or right multiplication with a non-singular matrix [28, Sec. 0.4.6 (b)], it is obvious that

$$\mathrm{rank}\left\{\bar{\mathbf{R}}\right\} = \mathrm{rank}\left\{\bar{\mathbf{R}}^{(\mathrm{p})}\right\} \tag{41}$$

$$\mathrm{rank}\left\{\mathbf{G}\right\} \leq 4 \tag{42}$$

hold. Moreover, we have $\mathrm{rank}\left\{\mathbf{A} \odot \mathbf{B}\right\} \leq \mathrm{rank}\left\{\mathbf{A}\right\}\mathrm{rank}\left\{\mathbf{B}\right\}$ [37, Th. 5.1.7] as well as $\mathrm{rank}\left\{\mathbf{A} \otimes \mathbf{B}\right\} = \mathrm{rank}\left\{\mathbf{A}\right\}\mathrm{rank}\left\{\mathbf{B}\right\}$ [37, Th. 4.2.15] for matrices $\mathbf{A}$ and $\mathbf{B}$ of appropriate sizes, and $\mathrm{rank}\left\{\mathbf{a}\mathbf{a}^H\right\} = 1$ holds for any column vector $\mathbf{a}$. With (36), (41), and (42), we then immediately obtain the inequality

$$\mathrm{rank}\left\{\bar{\mathbf{R}}\right\} \leq 4. \tag{43}$$

Appendix B
Rank of $\bar{\mathbf{R}}_{\mathrm{TX}}[m]$

We first drop the time argument to simplify notation. In order to evaluate the rank of $\bar{\mathbf{R}}_{\mathrm{TX}}$, we use $\mathbf{V}_{ab} = \mathbf{v}_{\mathrm{RX},ab}\mathbf{v}_{\mathrm{TX},ab}^T$ and $\boldsymbol{\Delta}_{\phi,ab} = \mathbf{d}_{\mathrm{RX},ab}\mathbf{d}_{\mathrm{TX},ab}^T$. Based on (4), we decompose the dominant channel component for each polarization combination $a,b \in \{\mathrm{V},\mathrm{H}\}$ as

$$\bar{\mathbf{H}}_{ab} = \left(\mathbf{v}_{\mathrm{RX},ab} \odot \mathbf{d}_{\mathrm{RX},ab}\right)\left(\mathbf{v}_{\mathrm{TX},ab} \odot \mathbf{d}_{\mathrm{TX},ab}\right)^T \; e^{j\phi_{ab}}. \tag{44}$$

We then obtain for $a,b,c,d \in \{\mathrm{V},\mathrm{H}\}$

$$\begin{aligned}\mathrm{E}\left\{\bar{\mathbf{H}}_{ab}^T\bar{\mathbf{H}}_{cd}^*\right\} &= \left(\mathbf{v}_{\mathrm{TX},ab} \odot \mathbf{d}_{\mathrm{TX},ab}\right)\left(\mathbf{v}_{\mathrm{TX},cd} \odot \mathbf{d}_{\mathrm{TX},cd}\right)^H f_{abcd} \\ f_{abcd} &= \left(\mathbf{v}_{\mathrm{RX},ab} \odot \mathbf{d}_{\mathrm{RX},ab}\right)^T \left(\mathbf{v}_{\mathrm{RX},cd} \odot \mathbf{d}_{\mathrm{RX},cd}\right)^* \\ &\quad \times \mathrm{E}\left\{e^{j(\phi_{ab}-\phi_{cd})}\right\}.\end{aligned} \tag{45}$$

With (2), we can write

$$\begin{aligned}&\bar{\mathbf{R}}_{\mathrm{TX}} \\ &= \mathrm{E}\left\{\begin{bmatrix} \bar{\mathbf{H}}_{\mathrm{VV}}^T\bar{\mathbf{H}}_{\mathrm{VV}}^* + \bar{\mathbf{H}}_{\mathrm{VH}}^T\bar{\mathbf{H}}_{\mathrm{VH}}^*, & \bar{\mathbf{H}}_{\mathrm{VV}}^T\bar{\mathbf{H}}_{\mathrm{HV}}^* + \bar{\mathbf{H}}_{\mathrm{VH}}^T\bar{\mathbf{H}}_{\mathrm{HH}}^* \\ \bar{\mathbf{H}}_{\mathrm{HV}}^T\bar{\mathbf{H}}_{\mathrm{VV}}^* + \bar{\mathbf{H}}_{\mathrm{HH}}^T\bar{\mathbf{H}}_{\mathrm{VH}}^*, & \bar{\mathbf{H}}_{\mathrm{HV}}^T\bar{\mathbf{H}}_{\mathrm{HV}}^* + \bar{\mathbf{H}}_{\mathrm{HH}}^T\bar{\mathbf{H}}_{\mathrm{HH}}^* \end{bmatrix}\right\}.\end{aligned} \tag{46}$$

Using (46) with (45), we obtain

$$\begin{aligned}\bar{\mathbf{R}}_{\mathrm{TX}} = &\begin{bmatrix}\begin{bmatrix}\mathbf{t}_{\mathrm{VV}} f_{\mathrm{VVVV}} \\ \mathbf{t}_{\mathrm{HV}} f_{\mathrm{HVVV}}\end{bmatrix}\mathbf{t}_{\mathrm{VV}}^H, & \begin{bmatrix}\mathbf{t}_{\mathrm{VV}} f_{\mathrm{VVHV}} \\ \mathbf{t}_{\mathrm{HV}} f_{\mathrm{HVHV}}\end{bmatrix}\mathbf{t}_{\mathrm{HV}}^H\end{bmatrix} \\ &+ \begin{bmatrix}\begin{bmatrix}\mathbf{t}_{\mathrm{VH}} f_{\mathrm{VHVH}} \\ \mathbf{t}_{\mathrm{HH}} f_{\mathrm{HHVH}}\end{bmatrix}\mathbf{t}_{\mathrm{VH}}^H, & \begin{bmatrix}\mathbf{t}_{\mathrm{VH}} f_{\mathrm{VHHH}} \\ \mathbf{t}_{\mathrm{HH}} f_{\mathrm{HHHH}}\end{bmatrix}\mathbf{t}_{\mathrm{HH}}^H\end{bmatrix}\end{aligned} \tag{47}$$

with $\mathbf{t}_{ab} = \mathbf{v}_{\mathrm{TX},ab} \odot \mathbf{d}_{\mathrm{TX},ab}$ for $a,b \in \{\mathrm{V},\mathrm{H}\}$. For matrices $\mathbf{A}$ and $\mathbf{B}$ of appropriate sizes, we have $\mathrm{rank}\left\{\mathbf{A}+\mathbf{B}\right\} \leq \mathrm{rank}\left\{\mathbf{A}\right\} + \mathrm{rank}\left\{\mathbf{B}\right\}$ [37, Sec. 0.4.5 (d)]. Thus, we conclude that

$$\mathrm{rank}\left\{\bar{\mathbf{R}}_{\mathrm{TX}}\right\} \leq 4 \tag{48}$$

must hold. If only the co-polarized sub-links have dominant components, $\mathrm{rank}\left\{\bar{\mathbf{R}}_{\mathrm{TX}}\right\} = 2$ is obtained using (47). For an SP setup with a dominant component, we have $\mathrm{rank}\left\{\bar{\mathbf{R}}_{\mathrm{TX}}\right\} = 1$.

Appendix C
Evaluation of the Fourth-Order Moment $\mathbf{T}[m]$

We now evaluate the fourth-order moment $\mathbf{T}[m] = \mathrm{E}\left\{\left(\mathbf{h}[m]\mathbf{h}^H[m]\right)^2\right\}$, where we drop the time argument for notational simplicity:

$$\begin{aligned}\mathbf{T} &= \mathrm{E}\left\{\left(\bar{\mathbf{h}}\bar{\mathbf{h}}^H + \tilde{\mathbf{h}}\tilde{\mathbf{h}}^H + \bar{\mathbf{h}}\tilde{\mathbf{h}}^H + \tilde{\mathbf{h}}\bar{\mathbf{h}}^H\right)^2\right\} \\ &\overset{(a)}{=} \mathrm{E}\left\{\bar{\mathbf{h}}\bar{\mathbf{h}}^H\bar{\mathbf{h}}\bar{\mathbf{h}}^H\right\} + \mathrm{E}\left\{\tilde{\mathbf{h}}\tilde{\mathbf{h}}^H\tilde{\mathbf{h}}\tilde{\mathbf{h}}^H\right\} + \bar{\mathbf{R}}\tilde{\mathbf{R}} + \tilde{\mathbf{R}}\bar{\mathbf{R}} \\ &\quad + \mathrm{E}\left\{\bar{\mathbf{h}}\,\mathrm{tr}\left\{\tilde{\mathbf{R}}\right\}\bar{\mathbf{h}}^H\right\} + \mathrm{E}\left\{\tilde{\mathbf{h}}\,\mathrm{tr}\left\{\bar{\mathbf{R}}\right\}\tilde{\mathbf{h}}^H\right\} \\ &\overset{(b)}{=} \bar{\mathbf{R}}\,\mathrm{tr}\left\{\bar{\mathbf{R}}\right\} + \tilde{\mathbf{R}}^2 + \tilde{\mathbf{R}}\,\mathrm{tr}\left\{\tilde{\mathbf{R}}\right\} + \bar{\mathbf{R}}\tilde{\mathbf{R}} \\ &\quad + \tilde{\mathbf{R}}\bar{\mathbf{R}} + \bar{\mathbf{R}}\,\mathrm{tr}\left\{\tilde{\mathbf{R}}\right\} + \tilde{\mathbf{R}}\,\mathrm{tr}\left\{\bar{\mathbf{R}}\right\} \\ &\overset{(c)}{=} \mathbf{R}\,\mathrm{tr}\left\{\mathbf{R}\right\} + \mathbf{R}^2 - \bar{\mathbf{R}}^2.\end{aligned} \tag{49}$$

In (a), we used $\mathrm{E}\left\{\bar{\mathbf{h}}\right\} = \mathbf{0}_{N_{\mathrm{TX}}N_{\mathrm{RX}},1}$, $\mathrm{E}\left\{\tilde{\mathbf{h}}\right\} = \mathbf{0}_{N_{\mathrm{TX}}N_{\mathrm{RX}},1}$, the mutual independency of $\bar{\mathbf{h}}$ and $\tilde{\mathbf{h}}$, and that $\mathrm{E}\left\{\tilde{\mathbf{h}}\tilde{\mathbf{h}}^T\right\} = \mathbf{0}_{N_{\mathrm{TX}}N_{\mathrm{RX}},N_{\mathrm{TX}}N_{\mathrm{RX}}}$ holds due to properness of $\tilde{\mathbf{h}}$. In (b), we made use of the fact that $\bar{\mathbf{h}}^H\bar{\mathbf{h}} = \mathrm{tr}\left\{\bar{\mathbf{R}}\right\}$, and we used [38, Th. 1] which yields the following identity for the zero-mean proper Gaussian random vector $\tilde{\mathbf{h}}$:

$$\begin{aligned}&\mathrm{E}\left\{\tilde{\mathbf{h}}\tilde{\mathbf{h}}^H\tilde{\mathbf{h}}\tilde{\mathbf{h}}^H\right\}\\&= \mathrm{E}\left\{\tilde{\mathbf{h}}\tilde{\mathbf{h}}^H\right\}\mathrm{E}\left\{\tilde{\mathbf{h}}\tilde{\mathbf{h}}^H\right\} + \mathrm{E}\left\{\tilde{\mathbf{h}}\,\mathrm{E}\left\{\tilde{\mathbf{h}}^H\tilde{\mathbf{h}}\right\}\tilde{\mathbf{h}}^H\right\}. \quad (50)\end{aligned}$$

In (c), we used $\mathbf{R} = \bar{\mathbf{R}} + \tilde{\mathbf{R}}$.

Appendix D
Sufficient Condition for a Positive Semidefinite $\tilde{\mathbf{R}}^{(e)}[m]$

In order to derive a sufficient condition for the positive semidefiniteness of $\breve{\mathbf{R}}_k[m], \forall k = 1, \ldots, N_{\mathrm{DP}}$ and thus $\tilde{\mathbf{R}}^{(e)}[m]$, we need to solve the following inequality for $c_k[m], \forall k = 1, \ldots, N_{\mathrm{DP}}$ for which we drop the time argument:

$$\mathbf{z}^H\left(\breve{\mathbf{R}}_{k-1} - c_k\ \breve{\mathbf{u}}_k\breve{\mathbf{u}}_k^H\right)\mathbf{z} \geq 0,\ \forall \mathbf{z} \in \mathbb{C}^{N_{\mathrm{TX}}N_{\mathrm{RX}}\times 1}. \quad (51)$$

The case $\mathbf{z} = \mathbf{0}_{N_{\mathrm{TX}}N_{\mathrm{RX}},1}$ is trivially satisfied. In case $\mathbf{z} \neq \mathbf{0}_{N_{\mathrm{TX}}N_{\mathrm{RX}},1}$, we first consider non-singular $\breve{\mathbf{R}}_{k-1}$. We define $\breve{\mathbf{z}} = \breve{\mathbf{R}}_{k-1}^{\frac{1}{2}}\mathbf{z}$ and rearrange (51) to obtain

$$\frac{c_k\ \mathbf{z}^H\breve{\mathbf{u}}_k\breve{\mathbf{u}}_k^H\mathbf{z}}{\mathbf{z}^H\breve{\mathbf{R}}_{k-1}\mathbf{z}} = \frac{c_k\ \breve{\mathbf{z}}^H\breve{\mathbf{R}}_{k-1}^{-\frac{1}{2}}\breve{\mathbf{u}}_k\breve{\mathbf{u}}_k^H\breve{\mathbf{R}}_{k-1}^{-\frac{1}{2}}\breve{\mathbf{z}}}{\breve{\mathbf{z}}^H\breve{\mathbf{z}}} \leq 1. \quad (52)$$

The matrix $\breve{\mathbf{R}}_{k-1}^{-\frac{1}{2}}\breve{\mathbf{u}}_k\breve{\mathbf{u}}_k^H\breve{\mathbf{R}}_{k-1}^{-\frac{1}{2}}$ is positive semidefinite with rank one such that, with the Rayleigh-Ritz theorem [28, Th. 4.2.2], we have

$$\begin{aligned}0 &\leq \frac{\breve{\mathbf{z}}^H\breve{\mathbf{R}}_{k-1}^{-\frac{1}{2}}\breve{\mathbf{u}}_k\breve{\mathbf{u}}_k^H\breve{\mathbf{R}}_{k-1}^{-\frac{1}{2}}\breve{\mathbf{z}}}{\breve{\mathbf{z}}^H\breve{\mathbf{z}}}\\&\leq \lambda_{\max}\left(\breve{\mathbf{R}}_{k-1}^{-\frac{1}{2}}\breve{\mathbf{u}}_k\breve{\mathbf{u}}_k^H\breve{\mathbf{R}}_{k-1}^{-\frac{1}{2}}\right). \quad (53)\end{aligned}$$

Finally, with (52) and (53), we obtain

$$\begin{aligned}c_k &\leq \lambda_{\max}^{-1}\left(\breve{\mathbf{R}}_{k-1}^{-\frac{1}{2}}\breve{\mathbf{u}}_k\breve{\mathbf{u}}_k^H\breve{\mathbf{R}}_{k-1}^{-\frac{1}{2}}\right)\\&= \left(\breve{\mathbf{u}}_k^H\breve{\mathbf{R}}_{k-1}^{-1}\breve{\mathbf{u}}_k\right)^{-1},\ \forall k = 1, \ldots, N_{\mathrm{DP}} \quad (54)\end{aligned}$$

which is a necessary and sufficient condition for $\breve{\mathbf{R}}_k, \forall k = 1, \ldots, N_{\mathrm{DP}}$ to be positive semidefinite if $\breve{\mathbf{R}}_{k-1}, \forall k = 1, \ldots, N_{\mathrm{DP}}$ is non-singular. In the case of a singular $\breve{\mathbf{R}}_{k-1}$, we set $c_k = 0$. We thus obtain a sufficient condition for $\tilde{\mathbf{R}}^{(e)}$ to be positive semidefinite. We note that (54) (for non-singular $\breve{\mathbf{R}}_{k-1}, \forall k = 1, \ldots, N_{\mathrm{DP}}$) can also be derived based on [28, Th. 7.7.7].

Appendix E
Approximate Evaluation of the MI

The approximate evaluation of the MI relies on a multivariate Taylor series expansion. We consider a complex function $f(\mathbf{a}, \mathbf{a}^*)$ with complex column vector arguments $\mathbf{a}$ and $\mathbf{a}^*$ of lengths N^2. We note that $\mathbf{a}^*$ is the complex conjugate of $\mathbf{a}$. The second-order approximation of $\mathbf{a}$ and $\mathbf{a}^*$ at $\mathbf{a}_0$ and $\mathbf{a}_0^*$, respectively, is given by [39]

$$\begin{aligned}f(\mathbf{a}, \mathbf{a}^*) \approx\ & f(\mathbf{a}_0, \mathbf{a}_0^*) + \left.\frac{\partial f}{\partial \mathbf{a}}\right|_{\mathbf{a}=\mathbf{a}_0, \mathbf{a}^*=\mathbf{a}_0^*} \cdot (\mathbf{a} - \mathbf{a}_0)\\&+ \left.\frac{\partial f}{\partial \mathbf{a}^*}\right|_{\mathbf{a}=\mathbf{a}_0, \mathbf{a}^*=\mathbf{a}_0^*} \cdot (\mathbf{a}^* - \mathbf{a}_0^*)\\&+\frac{1}{2}(\mathbf{a} - \mathbf{a}_0)^H \cdot \mathbf{H}_f^{cs}(\mathbf{a}_0, \mathbf{a}_0^*) \cdot (\mathbf{a} - \mathbf{a}_0)\\&+\frac{1}{2}(\mathbf{a} - \mathbf{a}_0)^T \cdot \mathbf{H}_f^{sc}(\mathbf{a}_0, \mathbf{a}_0^*) \cdot (\mathbf{a}^* - \mathbf{a}_0^*)\\&+\frac{1}{2}(\mathbf{a} - \mathbf{a}_0)^H \cdot \mathbf{H}_f^{cc}(\mathbf{a}_0, \mathbf{a}_0^*) \cdot (\mathbf{a}^* - \mathbf{a}_0^*)\\&+\frac{1}{2}(\mathbf{a} - \mathbf{a}_0)^T \cdot \mathbf{H}_f^{ss}(\mathbf{a}_0, \mathbf{a}_0^*) \cdot (\mathbf{a} - \mathbf{a}_0) \quad (55)\end{aligned}$$

with the row vector $\partial f/\partial \mathbf{a}$ defined by $[\partial f/\partial \mathbf{a}]_{1,k} = \partial f/\partial [\mathbf{a}]_{k,1}$ for $k = 1, \ldots, N$ and the $N^2 \times N^2$ Hessian matrices

$$\mathbf{H}_f^{cs}(\mathbf{a}_0, \mathbf{a}_0^*) = \left.\frac{\partial}{\partial \mathbf{a}}\left(\frac{\partial f}{\partial \mathbf{a}^*}\right)^T\right|_{\mathbf{a}=\mathbf{a}_0, \mathbf{a}^*=\mathbf{a}_0^*} \quad (56)$$

$$\mathbf{H}_f^{sc}(\mathbf{a}_0, \mathbf{a}_0^*) = \left(\mathbf{H}_f^{cs}(\mathbf{a}_0, \mathbf{a}_0^*)\right)^T \quad (57)$$

$$\mathbf{H}_f^{cc}(\mathbf{a}_0, \mathbf{a}_0^*) = \left.\frac{\partial}{\partial \mathbf{a}^*}\left(\frac{\partial f}{\partial \mathbf{a}^*}\right)^T\right|_{\mathbf{a}=\mathbf{a}_0, \mathbf{a}^*=\mathbf{a}_0^*} \quad (58)$$

$$\mathbf{H}_f^{ss}(\mathbf{a}_0, \mathbf{a}_0^*) = \left.\frac{\partial}{\partial \mathbf{a}}\left(\frac{\partial f}{\partial \mathbf{a}}\right)^T\right|_{\mathbf{a}=\mathbf{a}_0, \mathbf{a}^*=\mathbf{a}_0^*}. \quad (59)$$

We now consider the function

$$f(\mathbf{a}, \mathbf{a}^*) = f(\mathbf{a}) = \ln\det\mathbf{A} \quad (60)$$

with $\mathbf{a} = \mathrm{vec}\{\mathbf{A}\}$ and the $N \times N$ matrix $\mathbf{A}$. By using $f(\mathbf{a})$ in (55) with $\mathbf{a}_0 = \mathrm{E}\{\mathbf{a}\}$ and applying the expectation operator, we obtain the second-order approximation

$$\begin{aligned}&\mathrm{E}\{f(\mathbf{a})\} \approx f(\mathrm{E}\{\mathbf{a}\})\\&+\frac{1}{2}\mathrm{tr}\left\{\mathrm{E}\left\{(\mathbf{a} - \mathrm{E}\{\mathbf{a}\})(\mathbf{a} - \mathrm{E}\{\mathbf{a}\})^T\right\}\mathbf{H}_f^{ss}(\mathrm{E}\{\mathbf{a}\})\right\} \quad (61)\end{aligned}$$

where we used that only the first two and the last term in (55) are non-zero. The Hessian matrix $\mathbf{H}_f^{ss}(\mathrm{E}\{\mathbf{a}\}, \mathrm{E}\{\mathbf{a}^*\}) = \mathbf{H}_f^{ss}(\mathrm{E}\{\mathbf{a}\})$ is given by [40]

$$\mathbf{H}_f^{ss}(\mathrm{E}\{\mathbf{a}\}) = -\mathbf{K}_{N,N}\left((\mathrm{E}\{\mathbf{A}\})^{-T} \otimes (\mathrm{E}\{\mathbf{A}\})^{-1}\right). \quad (62)$$

For $\mathbf{A} = \mathbf{B} + \mathbf{CDE}$ with deterministic $N \times N$ matrices $\mathbf{B}$, $\mathbf{C}$, and $\mathbf{E}$, (61) can be written as

$$\begin{aligned}&\mathrm{E}\{f(\mathbf{a})\}\\&\overset{(a)}{\approx} f(\mathrm{E}\{\mathbf{a}\}) + \frac{1}{2}\mathrm{tr}\Big\{\left(\mathbf{E}^T \otimes \mathbf{C}\right)\\&\quad\times \mathrm{E}\left\{(\mathrm{vec}\{\mathbf{D} - \mathrm{E}\{\mathbf{D}\}\})(\mathrm{vec}\{\mathbf{D} - \mathrm{E}\{\mathbf{D}\}\})^T\right\}\\&\quad\times \left(\mathbf{E} \otimes \mathbf{C}^T\right)\mathbf{H}_f^{ss}(\mathrm{E}\{\mathbf{a}\})\Big\}\\&\overset{(b)}{=} f(\mathrm{E}\{\mathbf{a}\}) - \frac{1}{2}\mathrm{tr}\Big\{\left(\mathbf{E}^T \otimes \mathbf{C}\right)\\&\quad\times \mathrm{E}\left\{(\mathrm{vec}\{\mathbf{D} - \mathrm{E}\{\mathbf{D}\}\})(\mathrm{vec}\{\mathbf{D} - \mathrm{E}\{\mathbf{D}\}\})^T\right\}\mathbf{K}_{N,N}\\&\quad\times \left(\mathbf{C}^T \otimes \mathbf{E}\right)\left((\mathrm{E}\{\mathbf{A}\})^{-T} \otimes (\mathrm{E}\{\mathbf{A}\})^{-1}\right)\Big\}\end{aligned}$$

$$\overset{(c)}{=} f(\mathrm{E}\{\mathbf{a}\}) - \frac{1}{2} \times \mathrm{tr}\left\{ \mathrm{E}\left\{(\mathrm{vec}\{\mathbf{D}-\mathrm{E}\{\mathbf{D}\}\})(\mathrm{vec}\left\{\mathbf{D}^H-\mathrm{E}\left\{\mathbf{D}^H\right\}\right\})^H\right\} \times \left(\mathbf{E}\left(\mathrm{E}\{\mathbf{A}\}\right)^{-1}\mathbf{C}\right)^T \otimes \left(\mathbf{E}\left(\mathrm{E}\{\mathbf{A}\}\right)^{-1}\mathbf{C}\right)\right\}. \quad (63)$$

In (a), we applied $\mathrm{vec}\{\mathbf{CDE}\} = \left(\mathbf{E}^T \otimes \mathbf{C}\right)\mathrm{vec}\{\mathbf{D}\}$ [37, Lemma 4.3.1]. In (b), we inserted (62) and used $\left(\mathbf{E}\otimes\mathbf{C}^T\right)\mathbf{K}_{N,N} = \mathbf{K}_{N,N}\left(\mathbf{C}^T\otimes\mathbf{E}\right)$ [41, Th. 3.1 (viii)]. Finally, in (c), we used $\mathbf{K}_{N,N}^T = \mathbf{K}_{N,N}$ [41, Th. 3.1 (ii)] and $(\mathbf{A}\otimes\mathbf{B})(\mathbf{C}\otimes\mathbf{D}) = (\mathbf{AC})\otimes(\mathbf{BD})$ [37, Lemma 4.2.10].

Appendix F
Approximate Evaluation of the MI by Means of the Proposed Channel Model

We restate (20) as a function of the parameters obtained in the channel decomposition in Section III-C, i.e., $\bar{\mathbf{R}}[m]$ and $\tilde{\mathbf{R}}[m]$, only. To simplify notation, we drop the time argument for the remainder of this appendix. First, we rewrite (20):

$$\begin{aligned}\mathbf{Z} &\overset{(a)}{=} \mathrm{E}\left\{ \mathrm{vec}\left\{\bar{\mathbf{H}}^H\bar{\mathbf{H}}+\tilde{\mathbf{H}}^H\tilde{\mathbf{H}}+\bar{\mathbf{H}}^H\tilde{\mathbf{H}}+\tilde{\mathbf{H}}^H\bar{\mathbf{H}}\right\} \times \left(\mathrm{vec}\left\{\bar{\mathbf{H}}^H\bar{\mathbf{H}}+\tilde{\mathbf{H}}^H\tilde{\mathbf{H}}+\bar{\mathbf{H}}^H\tilde{\mathbf{H}}+\tilde{\mathbf{H}}^H\bar{\mathbf{H}}\right\}\right)^H \right\} \\ &\quad - \mathrm{vec}\left\{\bar{\mathbf{R}}_{\mathrm{TX}}^* + \tilde{\mathbf{R}}_{\mathrm{TX}}^*\right\}\left(\mathrm{vec}\left\{\bar{\mathbf{R}}_{\mathrm{TX}}^* + \tilde{\mathbf{R}}_{\mathrm{TX}}^*\right\}\right)^H \\ &\overset{(b)}{=} \mathrm{E}\left\{\mathrm{vec}\left\{\bar{\mathbf{H}}^H\bar{\mathbf{H}}\right\}\left(\mathrm{vec}\left\{\bar{\mathbf{H}}^H\bar{\mathbf{H}}\right\}\right)^H\right\} - \mathrm{vec}\left\{\bar{\mathbf{R}}_{\mathrm{TX}}^*\right\}\left(\mathrm{vec}\left\{\bar{\mathbf{R}}_{\mathrm{TX}}^*\right\}\right)^H \\ &\quad + \mathrm{E}\left\{\mathrm{vec}\left\{\tilde{\mathbf{H}}^H\tilde{\mathbf{H}}\right\}\left(\mathrm{vec}\left\{\tilde{\mathbf{H}}^H\tilde{\mathbf{H}}\right\}\right)^H\right\} - \mathrm{vec}\left\{\tilde{\mathbf{R}}_{\mathrm{TX}}^*\right\}\left(\mathrm{vec}\left\{\tilde{\mathbf{R}}_{\mathrm{TX}}^*\right\}\right)^H \\ &\quad + \mathrm{E}\left\{\mathrm{vec}\left\{\bar{\mathbf{H}}^H\tilde{\mathbf{H}}\right\}\left(\mathrm{vec}\left\{\bar{\mathbf{H}}^H\tilde{\mathbf{H}}\right\}\right)^H\right\} + \mathrm{E}\left\{\mathrm{vec}\left\{\tilde{\mathbf{H}}^H\bar{\mathbf{H}}\right\}\left(\mathrm{vec}\left\{\tilde{\mathbf{H}}^H\bar{\mathbf{H}}\right\}\right)^H\right\} \end{aligned} \quad (64)$$

with $\bar{\mathbf{R}}_{\mathrm{TX}} = \mathrm{E}\{\bar{\mathbf{H}}^T\bar{\mathbf{H}}^*\}$ and $\tilde{\mathbf{R}}_{\mathrm{TX}} = \mathrm{E}\{\tilde{\mathbf{H}}^T\tilde{\mathbf{H}}^*\}$. In (a), we applied $\mathbf{H} = \bar{\mathbf{H}}+\tilde{\mathbf{H}}$ and $\mathbf{R}_{\mathrm{TX}} = \bar{\mathbf{R}}_{\mathrm{TX}} + \tilde{\mathbf{R}}_{\mathrm{TX}}$. In (b), we used the properness of $\tilde{\mathbf{H}}$ to establish

$$\mathrm{E}\left\{\mathrm{vec}\left\{\bar{\mathbf{H}}^H\tilde{\mathbf{H}}\right\}\left(\mathrm{vec}\left\{\tilde{\mathbf{H}}^H\bar{\mathbf{H}}\right\}\right)^H\right\} = \mathbf{0}_{N_{\mathrm{TX}}^2,N_{\mathrm{TX}}^2}. \quad (65)$$

We now have

$$\begin{aligned}&\mathrm{E}\left\{\mathrm{vec}\left\{\tilde{\mathbf{H}}^H\bar{\mathbf{H}}\right\}\left(\mathrm{vec}\left\{\tilde{\mathbf{H}}^H\bar{\mathbf{H}}\right\}\right)^H\right\} \\ &\overset{(a)}{=} \mathrm{E}\left\{\left(\mathbf{I}_{N_{\mathrm{TX}}}\otimes\tilde{\mathbf{H}}^H\right)\mathrm{vec}\{\bar{\mathbf{H}}\}\left(\mathrm{vec}\{\bar{\mathbf{H}}\}\right)^H\left(\mathbf{I}_{N_{\mathrm{TX}}}\otimes\tilde{\mathbf{H}}\right)\right\} \\ &= \mathrm{E}\left\{\left(\mathbf{I}_{N_{\mathrm{TX}}}\otimes\tilde{\mathbf{H}}^H\right)\bar{\mathbf{R}}\left(\mathbf{I}_{N_{\mathrm{TX}}}\otimes\tilde{\mathbf{H}}\right)\right\} \end{aligned} \quad (66)$$

where, in (a), we used [37, Lemma 4.3.1]. Similarly, we have

$$\begin{aligned}&\mathrm{E}\left\{\mathrm{vec}\left\{\bar{\mathbf{H}}^H\tilde{\mathbf{H}}\right\}\left(\mathrm{vec}\left\{\bar{\mathbf{H}}^H\tilde{\mathbf{H}}\right\}\right)^H\right\} \\ &\overset{(a)}{=} \left(\mathrm{E}\left\{\left(\tilde{\mathbf{H}}^H\otimes\mathbf{I}_{N_{\mathrm{TX}}}\right)\mathbf{K}_{N_{\mathrm{TX}},N_{\mathrm{TX}}}\mathrm{vec}\{\bar{\mathbf{H}}\}\left(\mathrm{vec}\{\bar{\mathbf{H}}\}\right)^H \times \mathbf{K}_{N_{\mathrm{TX}},N_{\mathrm{TX}}}\left(\tilde{\mathbf{H}}\otimes\mathbf{I}_{N_{\mathrm{TX}}}\right)\right\}\right)^* \\ &\overset{(b)}{=} \mathbf{K}_{N_{\mathrm{TX}},N_{\mathrm{TX}}}\left(\mathrm{E}\left\{\left(\mathbf{I}_{N_{\mathrm{TX}}}\otimes\tilde{\mathbf{H}}^H\right)\bar{\mathbf{R}}\left(\mathbf{I}_{N_{\mathrm{TX}}}\otimes\tilde{\mathbf{H}}\right)\right\}\right)^* \times \mathbf{K}_{N_{\mathrm{TX}},N_{\mathrm{TX}}} \end{aligned} \quad (67)$$

where, in (a), we used [41, Th. 3.1 (ii)], and, in (b), we used [41, Th. 3.1 (viii)]. Next, we have

$$\begin{aligned}&\mathrm{E}\left\{\mathrm{vec}\left\{\tilde{\mathbf{H}}^H\tilde{\mathbf{H}}\right\}\left(\mathrm{vec}\left\{\tilde{\mathbf{H}}^H\tilde{\mathbf{H}}\right\}\right)^H\right\} \\ &\overset{(a)}{=} \mathrm{E}\left\{\left(\mathbf{I}_{N_{\mathrm{TX}}}\otimes\tilde{\mathbf{H}}^H\right)\mathrm{vec}\left\{\tilde{\mathbf{H}}\right\}\right\} \times \mathrm{E}\left\{\left(\mathrm{vec}\left\{\tilde{\mathbf{H}}\right\}\right)^H\left(\mathbf{I}_{N_{\mathrm{TX}}}\otimes\tilde{\mathbf{H}}^H\right)^H\right\} \\ &\quad + \mathrm{E}\left\{\left(\mathbf{I}_{N_{\mathrm{TX}}}\otimes\tilde{\mathbf{H}}^H\right)\tilde{\mathbf{R}}\left(\mathbf{I}_{N_{\mathrm{TX}}}\otimes\tilde{\mathbf{H}}\right)\right\} \\ &= \mathrm{vec}\left\{\tilde{\mathbf{R}}_{\mathrm{TX}}^*\right\}\left(\mathrm{vec}\left\{\tilde{\mathbf{R}}_{\mathrm{TX}}^*\right\}\right)^H + \mathrm{E}\left\{\left(\mathbf{I}_{N_{\mathrm{TX}}}\otimes\tilde{\mathbf{H}}^H\right)\tilde{\mathbf{R}}\left(\mathbf{I}_{N_{\mathrm{TX}}}\otimes\tilde{\mathbf{H}}\right)\right\} \end{aligned} \quad (68)$$

where, in (a), we used [38, Th. 1] with the properness of $\tilde{\mathbf{H}}$. In order to evaluate (66), (67), and (68), we use that

$$\begin{aligned}&\mathrm{vec}\left\{\mathrm{E}\left\{\left(\mathbf{I}_{N_{\mathrm{TX}}}\otimes\tilde{\mathbf{H}}^H\right)\mathbf{A}\left(\mathbf{I}_{N_{\mathrm{TX}}}\otimes\tilde{\mathbf{H}}\right)\right\}\right\} \\ &= \left(\mathbf{I}_{N_{\mathrm{TX}}}\otimes\mathrm{E}\left\{\tilde{\mathbf{H}}^T\otimes\mathbf{I}_{N_{\mathrm{TX}}}\otimes\tilde{\mathbf{H}}^H\right\}\right)\mathrm{vec}\{\mathbf{A}\} \\ &= (\mathbf{I}_{N_{\mathrm{TX}}}\otimes\mathbf{Y})\,\mathrm{vec}\{\mathbf{A}\} \end{aligned} \quad (69)$$

holds for a deterministic $N_{\mathrm{TX}}N_{\mathrm{RX}}\times N_{\mathrm{TX}}N_{\mathrm{RX}}$ matrix $\mathbf{A}$. Here, the $N_{\mathrm{TX}}^3 \times N_{\mathrm{TX}}N_{\mathrm{RX}}^2$ block matrix $\mathbf{Y}$ contains $\mathbf{I}_{N_{\mathrm{TX}}}\otimes\mathbf{X}_{k,l}$ in the kth row-partition and the lth column-partition for $k = 1,\ldots,N_{\mathrm{TX}}$ and $l = 1,\ldots,N_{\mathrm{RX}}$. The $N_{\mathrm{TX}}\times N_{\mathrm{RX}}$ matrix $\mathbf{X}_{k,l}$ is defined by $\left[\mathbf{X}_{k,l}\right]_{p,q} = \left[\tilde{\mathbf{R}}\right]_{(k-1)N_{\mathrm{RX}}+l,(p-1)N_{\mathrm{RX}}+q}$ for $p = 1,\ldots,N_{\mathrm{TX}}$ and $q = 1,\ldots,N_{\mathrm{RX}}$. For the DP case where only the co-polarized sub-links can be affected by dominant components, we can write $\bar{\mathbf{H}} = \bar{\mathbf{H}}_1 + \bar{\mathbf{H}}_2$ with

$$\bar{\mathbf{H}}_1 = \begin{bmatrix} \bar{\mathbf{H}}_{\mathrm{VV}} & \mathbf{0}_{\frac{N_{\mathrm{RX}}}{2},\frac{N_{\mathrm{TX}}}{2}} \\ \mathbf{0}_{\frac{N_{\mathrm{RX}}}{2},\frac{N_{\mathrm{TX}}}{2}} & \mathbf{0}_{\frac{N_{\mathrm{RX}}}{2},\frac{N_{\mathrm{TX}}}{2}} \end{bmatrix} \quad (70)$$

$$\bar{\mathbf{H}}_2 = \begin{bmatrix} \mathbf{0}_{\frac{N_{\mathrm{RX}}}{2},\frac{N_{\mathrm{TX}}}{2}} & \mathbf{0}_{\frac{N_{\mathrm{RX}}}{2},\frac{N_{\mathrm{TX}}}{2}} \\ \mathbf{0}_{\frac{N_{\mathrm{RX}}}{2},\frac{N_{\mathrm{TX}}}{2}} & \bar{\mathbf{H}}_{\mathrm{HH}} \end{bmatrix}. \quad (71)$$

Obviously, we have $\bar{\mathbf{H}}_1^H\bar{\mathbf{H}}_2 = \mathbf{0}_{N_{\mathrm{TX}},N_{\mathrm{TX}}}$ and $\bar{\mathbf{H}}^H\bar{\mathbf{H}} = \bar{\mathbf{H}}_1^H\bar{\mathbf{H}}_1 + \bar{\mathbf{H}}_2^H\bar{\mathbf{H}}_2$. Furthermore, with (4), we have $\bar{\mathbf{R}}_{\mathrm{TX}}^* = \mathrm{E}\left\{\bar{\mathbf{H}}_1^H\bar{\mathbf{H}}_1 + \bar{\mathbf{H}}_2^H\bar{\mathbf{H}}_2\right\} = \bar{\mathbf{H}}^H\bar{\mathbf{H}}$. It thus follows that

$$\begin{aligned}&\mathrm{E}\left\{\mathrm{vec}\left\{\bar{\mathbf{H}}^H\bar{\mathbf{H}}\right\}\left(\mathrm{vec}\left\{\bar{\mathbf{H}}^H\bar{\mathbf{H}}\right\}\right)^H\right\} \\ &= \mathrm{vec}\left\{\bar{\mathbf{R}}_{\mathrm{TX}}^*\right\}\left(\mathrm{vec}\left\{\bar{\mathbf{R}}_{\mathrm{TX}}^*\right\}\right)^H. \end{aligned} \quad (72)$$

Clearly, the same result holds in the SP case. At last, using (64) with (66), (67), (68), (69), and (72), we obtain the result in (21).

APPENDIX G
LOWER BOUND ON THE APPROXIMATE EVALUATION OF THE MI

In order to lower-bound the approximate MI (19), we find an upper bound for the trace in the second term of (19) for the case that the eigenvectors of $\mathbf{R}_{\text{TX}}^*[m]$ form the precoding for N_{st} transmitted streams. We drop the time argument in the following derivation. Using the eigendecompositions $\mathbf{R}_{\text{TX}}^* = \mathbf{U}_{\text{TX}}\mathbf{\Lambda}_{\text{TX}}\mathbf{U}_{\text{TX}}^H$ and $\mathbf{Q} = \mathbf{U}_{\text{TX}}\mathbf{\Lambda}_Q\mathbf{U}_{\text{TX}}^H$, we can write

$$\begin{aligned}
&\operatorname{tr}\Bigg\{\mathbf{Z}\Bigg(\left(\mathbf{Q}\left(\mathbf{I}_{N_{\text{TX}}}+\rho\mathbf{R}_{\text{TX}}^*\mathbf{Q}\right)^{-1}\right)^T \\
&\quad\otimes\left(\mathbf{Q}\left(\mathbf{I}_{N_{\text{TX}}}+\rho\mathbf{R}_{\text{TX}}^*\mathbf{Q}\right)^{-1}\right)\Bigg)\Bigg\} \\
&\overset{\text{(a)}}{=}\operatorname{tr}\Bigg\{\mathbf{Z}(\mathbf{U}_{\text{TX}}^*\otimes\mathbf{U}_{\text{TX}})\Bigg(\left(\mathbf{\Lambda}_Q\left(\mathbf{I}_{N_{\text{TX}}}+\rho\mathbf{\Lambda}_{\text{TX}}\mathbf{\Lambda}_Q\right)^{-1}\right)^T \\
&\quad\otimes\left(\mathbf{\Lambda}_Q\left(\mathbf{I}_{N_{\text{TX}}}+\rho\mathbf{\Lambda}_{\text{TX}}\mathbf{\Lambda}_Q\right)^{-1}\right)\Bigg)(\mathbf{U}_{\text{TX}}^T\otimes\mathbf{U}_{\text{TX}}^H)\Bigg\} \\
&\overset{\text{(b)}}{=}\operatorname{tr}\Bigg\{\mathbf{Z}^{(U)}\odot\Bigg(\left(\mathbf{\Lambda}_Q\left(\mathbf{I}_{N_{\text{TX}}}+\rho\mathbf{\Lambda}_{\text{TX}}\mathbf{\Lambda}_Q\right)^{-1}\right)^T \\
&\quad\otimes\left(\mathbf{\Lambda}_Q\left(\mathbf{I}_{N_{\text{TX}}}+\rho\mathbf{\Lambda}_{\text{TX}}\mathbf{\Lambda}_Q\right)^{-1}\right)\Bigg)\Bigg\} \\
&\overset{\text{(c)}}{=}\sum_{k=1}^{N_{\text{st}}}\sum_{l=1}^{N_{\text{st}}}\frac{\left[\mathbf{Z}^{(U)}\right]_{(k-1)N_{\text{TX}}+l,(k-1)N_{\text{TX}}+l}\ \lambda_{Q,k}\lambda_{Q,l}}{\left(1+\rho\lambda_{\text{TX},k}\lambda_{Q,k}\right)\left(1+\rho\lambda_{\text{TX},l}\lambda_{Q,l}\right)} \\
&\overset{\text{(d)}}{\leq}\frac{1}{\rho^2}\sum_{k=1}^{N_{\text{st}}}\sum_{l=1}^{N_{\text{st}}}\frac{\left[\mathbf{Z}^{(U)}\right]_{(k-1)N_{\text{TX}}+l,(k-1)N_{\text{TX}}+l}}{\lambda_{\text{TX},k}\lambda_{\text{TX},l}}
\end{aligned}\tag{73}$$

with

$$\mathbf{Z}^{(U)} = (\mathbf{U}_{\text{TX}}^T\otimes\mathbf{U}_{\text{TX}}^H)\mathbf{Z}(\mathbf{U}_{\text{TX}}^*\otimes\mathbf{U}_{\text{TX}}).\tag{74}$$

In (a), we used [37, Lemma 4.2.10] as in (63). In (b), we applied the identity $\operatorname{tr}\{\mathbf{AD}\} = \operatorname{tr}\{\mathbf{A}\odot\mathbf{D}\}$ for matrices $\mathbf{A}$ and $\mathbf{D}$ of appropriate sizes, where $\mathbf{D}$ is diagonal. In (c), we made use of the fact that only the first N_{st} elements on the diagonal of $\mathbf{\Lambda}_Q$ are non-zero. Finally, for (d), we note that $\mathbf{Z}^{(U)}$ is positive semidefinite.

REFERENCES

[1] M. Coldrey, "Modeling and capacity of polarized MIMO channels," in *Proc. 67th IEEE Veh. Technol. Conf. (VTC)*, Singapore, May 2008, pp. 440–444.

[2] C. Oestges, B. Clerckx, M. Guillaud, and M. Debbah, "Dual-polarized wireless communications: From propagation models to system performance evaluation," *IEEE Trans. Wireless Commun.*, vol. 7, no. 10, pp. 4019–4031, Oct. 2008.

[3] V. Erceg, P. Soma, D. S. Baum, and S. Catreux, "Multiple-input multiple-output fixed wireless radio channel measurements and modeling using dual-polarized antennas at 2.5 GHz," *IEEE Trans. Wireless Commun.*, vol. 3, no. 6, pp. 2288–2298, Nov. 2004.

[4] V. Degli-Esposti, V.-M. Kolmonen, E. M. Vitucci, and P. Vainikainen, "Analysis and modeling on co- and cross-polarized urban radio propagation for dual-polarized MIMO wireless systems," *IEEE Trans. Antennas Propag.*, vol. 59, no. 11, pp. 4247–4256, Nov. 2011.

[5] F. Quitin, C. Oestges, F. Horlin, and P. De Doncker, "Polarization measurements and modeling in indoor NLOS environments," *IEEE Trans. Wireless Commun.*, vol. 9, no. 1, pp. 21–25, Jan. 2010.

[6] M. Landmann, K. Sivasondhivat, J.-I. Takada, I. Ida, and R. Thomä, "Polarization behavior of discrete multipath and diffuse scattering in urban environments at 4.5 GHz," *EURASIP J. Wireless Commun. and Networking*, vol. 2007, no. 1, Jan. 2007.

[7] R. Tian, B. K. Lau, and J. Medbo, "Impact of Rician fading on the orthogonality of dual-polarized macrocellular channels," in *Proc. 6th European Conf. Antennas and Propagation (EUCAP)*, Prague, Czech Republic, Mar. 2012, pp. 447–451.

[8] R. Nabar, H. Bölcskei, and A. Paulraj, "Diversity and outage performance in space-time block coded Ricean MIMO channels," *IEEE Trans. Wireless Commun.*, vol. 4, no. 5, pp. 2519–2532, Sep. 2005.

[9] C. Oestges, "Channel correlations and capacity metrics in MIMO dual-polarized Rayleigh and Ricean channels," in *Proc. 60th IEEE Veh. Technol. Conf. (VTC)*, Los Angeles, CA, USA, Sep. 2004, pp. 1453–1457.

[10] G. Taricco, "Further results on the asymptotic mutual information of Rician fading MIMO channels," *IEEE Trans. Inf. Theory*, vol. 59, no. 2, pp. 894–915, Feb. 2013.

[11] V. R. Anreddy and M. A. Ingram, "Capacity of measured Ricean and Rayleigh indoor MIMO channels at 2.4 GHz with polarization and spatial diversity," in *Proc. IEEE Conf. Wireless Commun. and Networking (WCNC)*, Las Vegas, NV, USA, Apr. 2006, pp. 946–951.

[12] P. Kyritsi, D. C. Cox, R. A. Valenzuela, and P. W. Wolniansky, "Effect of antenna polarization on the capacity of a multiple element system in an indoor environment," *IEEE J. Sel. Areas Commun.*, vol. 20, no. 6, pp. 1227–1239, Aug. 2002.

[13] V. Erceg, H. Sampath, and S. Catreux-Erceg, "Dual-polarization versus single-polarization MIMO channel measurement results and modeling," *IEEE Trans. Wireless Commun.*, vol. 5, no. 1, pp. 28–33, Jan. 2006.

[14] V. Raghavan, A. M. Sayeed, and V. V. Veeravalli, "Semiunitary precoding for spatially correlated MIMO channels," *IEEE Trans. Inf. Theory*, vol. 57, no. 3, pp. 1284–1298, Mar. 2011.

[15] T. Kim, B. Clerckx, D. J. Love, and S. J. Kim, "Limited feedback beamforming systems for dual-polarized MIMO channels," *IEEE Trans. Wireless Commun.*, vol. 9, no. 11, pp. 3425–3439, Nov. 2010.

[16] B. Clerckx, Y. Zhou, and S. Kim, "Practical codebook design for limited feedback spatial multiplexing," in *Proc. IEEE Int. Conf. Commun. (ICC)*, Beijing, China, May 2008, pp. 3982–3987.

[17] J. Choi, B. Clerckx, and D. Love, "Differential codebook for general rotated dual-polarized MISO channels," in *Proc. IEEE Global Commun. Conf. (GLOBECOM)*, Anaheim, CA, USA, Dec. 2012.

[18] P. Almers, E. Bonek, A. Burr, N. Czink, M. Debbah, V. Degli-Esposti, H. Hofstetter, P. Kyösti, D. Laurenson, G. Matz, A. F. Molisch, C. Oestges, and H. Özcelik, "Survey of channel and radio propagation models for wireless MIMO systems," *EURASIP J. Wireless Commun. and Networking*, vol. 2007, no. 1, Jan. 2007.

[19] M. Narandžić, M. Käske, C. Schneider, M. Milojević, M. Landmann, G. Sommerkorn, and R. S. Thomä, "3D-antenna array model for IST-WINNER channel simulations," in *Proc. 65th IEEE Veh. Technol. Conf. (VTC)*, Dublin, Ireland, Apr. 2007, pp. 319–323.

[20] S. Jaeckel, K. Börner, L. Thiele, and V. Jungnickel, "A geometric polarization rotation model for the 3-D spatial channel model," *IEEE Trans. Antennas Propag.*, vol. 60, no. 12, pp. 5966–5977, Dec. 2012.

[21] S. Jin, X. Gao, and X. You, "On the ergodic capacity of rank-1 Ricean-fading MIMO channels," *IEEE Trans. Inf. Theory*, vol. 53, no. 2, pp. 502–517, Feb. 2007.

[22] F. R. Farrokhi, G. J. Foschini, A. Lozano, and R. A. Valenzuela, "Link-optimal space-time processing with multiple transmit and receive antennas," *IEEE Commun. Lett.*, vol. 5, no. 3, pp. 85–87, Mar. 2001.

[23] S. Wyne, A. F. Molisch, P. Almers, G. Eriksson, J. Karedal, and F. Tufvesson, "Statistical evaluation of outdoor-to-indoor office MIMO measurements at 5.2 GHz," in *Proc. 61st IEEE Veh. Technol. Conf. (VTC)*, Stockholm, Sweden, May 2005, pp. 146–150.

[24] F. Quitin, F. Bellens, A. Panahandeh, J.-M. Dricot, F. Dossin, F. Horlin, C. Oestges, and P. De Doncker, "A time-variant statistical channel model for tri-polarized antenna systems," in *Proc. 21st IEEE Int. Symp. Personal, Indoor and Mobile Radio Commun. (PIMRC)*, Istanbul, Turkey, Sep. 2010, pp. 64–69.

[25] L. J. Greenstein, D. G. Michelson, and V. Erceg, "Moment-method estimation of the Ricean K-factor," *IEEE Commun. Lett.*, vol. 3, no. 6, pp. 175–176, Jun. 1999.

[26] M. Landmann, M. Käske, and R. S. Thomä, "Impact of incomplete and inaccurate data models on high resolution parameter estimation in multidimensional channel sounding," *IEEE Trans. Antennas Propag.*, vol. 60, no. 2, pp. 557–573, Feb. 2012.

[27] G. H. Golub and C. F. Van Loan, *Matrix Computations*. Baltimore, MD, USA: The Johns Hopkins Univ. Press, 1996.

[28] R. A. Horn and C. R. Johnson, *Matrix Analysis*. Cambridge, UK: Cambridge Univ. Press, 1990.

[29] A. Ispas, C. Schneider, G. Ascheid, and R. Thomä, "Performance evaluation of downlink beamforming over non-stationary channels with

interference," in *Proc. 22nd IEEE Int. Symp. Personal, Indoor and Mobile Radio Commun. (PIMRC)*, Toronto, Canada, Sep. 2011, pp. 1677–1681.
[30] A. Lozano and N. Jindal, "Are yesterday's information-theoretic fading models and performance metrics adequate for the analysis of today's wireless systems?" *IEEE Commun. Mag.*, vol. 50, no. 11, pp. 210–217, Nov. 2012.
[31] C. Schneider, C. Jandura, G. Sommerkorn, M. Narandžić, M. Käske, A. Hong, V. Algeier, W. A. Kotterman, and R. S. Thomä, "Multi-user MIMO channel reference data for channel modelling and system evaluation from measurements," in *Proc. Int. ITG Workshop Smart Antennas (WSA)*, Berlin, Germany, Feb. 2009.
[32] A. Ispas, C. Schneider, G. Ascheid, and R. Thomä, "Analysis of local quasi-stationarity regions in an urban macrocell scenario," in *Proc. 71st IEEE Veh. Technol. Conf. (VTC)*, Taipei, Taiwan, May 2010.
[33] L. Jiang, V. Jungnickel, S. Jaeckel, L. Thiele, and A. Brylka, "Correlation analysis of multiple-input multiple-output channels with cross-polarized antennas," in *Proc. 14th Asia-Pacific Conf. Commun. (APCC)*, Tokyo, Japan, Oct. 2008.
[34] V. Erceg, P. Soma, D. S. Baum, and A. J. Paulraj, "Capacity obtained from multiple-input multiple-output channel measurements in fixed wireless environments at 2.5 GHz," in *Proc. IEEE Int. Conf. Commun. (ICC)*, New York, NY, USA, Apr. 2002, pp. 396–400.
[35] C. Schneider and R. S. Thomä, "Evaluation of LTE link-level performance with closed loop spatial multiplexing in a realistic urban macro environment," in *Proc. 6th European Conf. Antennas and Propagation (EUCAP)*, Prague, Czech Republic, Mar. 2012, pp. 2725–2729.
[36] M. Vu and A. Paulraj, "On the capacity of MIMO wireless channels with dynamic CSIT," *IEEE J. Sel. Areas Commun.*, vol. 25, no. 7, pp. 1269–1283, Sep. 2007.
[37] R. A. Horn and C. R. Johnson, *Topics in Matrix Analysis*. Cambridge, UK: Cambridge Univ. Press, 1994.
[38] P. H. M. Janssen and P. Stoica, "On the expectation of the product of four matrix-valued Gaussian random variables," *IEEE Trans. Autom. Control*, vol. 33, no. 9, pp. 867–870, Sep. 1988.
[39] A. Hjørungnes, *Complex-Valued Matrix Derivatives: With Applications in Signal Processing and Communications*. Cambridge, UK: Cambridge Univ. Press, 2011.
[40] A. Hjørungnes and D. Gesbert, "Complex-valued matrix differentiation: Techniques and key results," *IEEE Trans. Signal Process.*, vol. 55, no. 6, pp. 2740–2746, Jun. 2007.
[41] J. R. Magnus and H. Neudecker, "The commutation matrix: Some properties and applications," *Ann. Stat.*, vol. 7, no. 2, pp. 381–394, Mar. 1979.

Adrian Ispas (S'11) obtained the Dipl.-Ing. degree in electrical engineering and information technology (with distinction) from RWTH Aachen University, Germany, in 2007. He is currently pursuing a doctorate degree at the Chair for Integrated Signal Processing Systems, RWTH Aachen University. Since 2013, he has been with Rohde & Schwarz GmbH & Co. KG, Munich, Germany. His main research interests lie in the areas of signal processing and channel modeling/characterization.

Adrian Ispas received the Henry Ford II Award 2005 for academic achievements during his studies and the SEW-EURODRIVE-Stiftung Award 2008 in recognition of his diploma thesis.

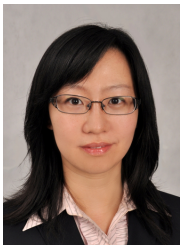

Xitao Gong (S'09) received the bachelor and master degrees from Southeast University, China in 2004 and 2007, respectively. She is currently working as a research assistant and pursuing a doctorate degree at the Chair for Integrated Signal Processing Systems, RWTH Aachen University. Her main research interests are interference detection and mitigation in cognitive and cooperative networks.

Christian Schneider received his Diploma degree in electrical engineering from the Ilmenau University of Technology, Ilmenau, Germany in 2001. He is currently pursuing the Dr.-Ing. degree with the Institute for Information Technology at the Ilmenau University of Technology.

His research interests include space-time signal processing, turbo techniques, adaptive techniques, multi dimensional channel sounding, channel characterization and analysis as well as channel modelling for single and multi-user cases.

Gerd Ascheid (SM'08) received his Diploma and PhD degrees in Electrical Engineering from RWTH Aachen University. In 1988 he started as a co-founder and managing director CADIS GmbH which successfully brought the system simulation tool COSSAP to the market. In 1994 CADIS was acquired by Synopsys Inc., a California-based EDA market leader. From 1994-2003 Gerd Ascheid worked as Director/Senior Director with Synopsys. In 2002 he was co-founder of LisaTek GmbH whose processor design tools are now part of the Synopsys product portfolio. In 2003 Gerd Ascheid joined RWTH Aachen University as a professor for Integrated Signal Processing Systems. He is also coordinator of the UMIC (Ultra-high speed Mobile Information and Communication) Research Centre at RWTH Aachen University. His research interest is in wireless communication algorithms, application specific integrated platforms, in particular, for mobile terminals and cyber physical devices.

Reiner Thomä (M'92–SM'99–F'07) received the Dipl.-Ing. (M.S.E.E.), Dr.-Ing. (Ph.D.E.E.), and the Dr.-Ing. habil. degrees in electrical engineering and information technology from Technische Hochschule Ilmenau, Germany, in 1975, 1983, and 1989, respectively.

From 1975 to 1988, he was a Research Associate in the fields of electronic circuits, measurement engineering, and digital signal processing at the same university. From 1988 to 1990, he was a Research Engineer at the Akademie der Wissenschaften der DDR (Zentrum für Wissenschaftlichen Gerätebau). During this period he was working in the field of radio surveillance. In 1991, he spent a three-month sabbatical leave at the University of Erlangen-Nürnberg (Lehrstuhl für Nachrichtentechnik). Since 1992, he has been a Professor of electrical engineering (electronic measurement) at TU Ilmenau where he was the Director of the Institute of Communications and Measurement Engineering from 1999 until 2005. With his group, he has contributed to several European and German research projects and clusters such as WINNER, PULSERS, EUWB, NEWCOM, COST 273, 2100, IC 1004, EASY-A, EASY-C. Currently he is the speaker of the German nation-wide DFG-focus project UKoLOS, Ultra-Wideband Radio Technologies for Communications, Localization and Sensor Applications (SPP 1202). His research interests include measurement and digital signal processing methods (correlation and spectral analysis, system identification, sensor arrays, compressive sensing, time-frequency and cyclostationary signal analysis), their application in mobile radio and radar systems (multidimensional channel sounding, propagation measurement and parameter estimation, MIMO-, mm-wave-, and ultra-wideband radar), measurement-based performance evaluation of MIMO transmission systems including over-the-air testing in virtual electromagnetic environments, and UWB sensor systems for object detection, tracking and imaging.

Prof. Thomä is a member of URSI (Comm. A), VDE/ITG. Since 1999 he has been serving as chair of the IEEE-IM TC-13 on Measurement in Wireless and Telecommunications. In 2007 he was awarded IEEE Fellow Member and received the Thuringian State Research Award for Applied Research both for contributions to high-resolution multidimensional channel sounding.